NAVAL POSTGRADUATE SCHOOL

MONTEREY, CALIFORNIA

THESIS

SYSTEMATIC REVIEW OF ULTRASONIC IMPACT
TREATMENT PARAMETERS ON RESIDUAL
STRESSES OF WELDED NON-SENSITIZED VERSUS
SENSITIZED ALUMINUM-MAGNESIUM

by

Eid Faiz Fakhouri

March 2015

Thesis Advisor: Sarath Menon
Co-Advisor: Luke N. Brewer

Approved for public release; distribution is unlimited

THIS PAGE INTENTIONALLY LEFT BLANK

REPORT DOCUMENTATION PAGE		*Form Approved OMB No. 0704–0188*
Public reporting burden for this collection of information is estimated to average 1 hour per response, including the time for reviewing instruction, searching existing data sources, gathering and maintaining the data needed, and completing and reviewing the collection of information. Send comments regarding this burden estimate or any other aspect of this collection of information, including suggestions for reducing this burden, to Washington headquarters Services, Directorate for Information Operations and Reports, 1215 Jefferson Davis Highway, Suite 1204, Arlington, VA 22202-4302, and to the Office of Management and Budget, Paperwork Reduction Project (0704-0188) Washington, DC 20503.		
1. AGENCY USE ONLY *(Leave blank)*	**2. REPORT DATE** March 2015	**3. REPORT TYPE AND DATES COVERED** Master's Thesis
4. TITLE AND SUBTITLE SYSTEMATIC REVIEW OF ULTRASONIC IMPACT TREATMENT PARAMETERS ON RESIDUAL STRESSES OF WELDED NON-SENSITIZED VERSUS SENSITIZED ALUMINUM-MAGNESIUM		**5. FUNDING NUMBERS**
6. AUTHOR(S) Eid Faiz Fakhouri		
7. PERFORMING ORGANIZATION NAME(S) AND ADDRESS(ES) Naval Postgraduate School Monterey, CA 93943-5000		**8. PERFORMING ORGANIZATION REPORT NUMBER**
9. SPONSORING /MONITORING AGENCY NAME(S) AND ADDRESS(ES) N/A		**10. SPONSORING/MONITORING AGENCY REPORT NUMBER**
11. SUPPLEMENTARY NOTES The views expressed in this thesis are those of the author and do not reflect the official policy or position of the Department of Defense or the U.S. Government. IRB Protocol number ____N/A____.		
12a. DISTRIBUTION / AVAILABILITY STATEMENT Approved for public release; distribution is unlimited		**12b. DISTRIBUTION CODE** A

13. ABSTRACT (maximum 200 words)

This thesis focuses on the use of x-ray diffraction to measure residual stresses around welds in 5XXX series aluminum-alloys used in naval ship structures both in the laboratory and the field. Tensile residual stresses are commonly generated during welding and, in sensitized alloys, can cause stress corrosion cracking. Peening techniques, such as ultrasonic impact treatment (UIT), can mitigate and possibly reverse these tensile residual stresses. This research uses x-ray diffraction to measure residual stresses around welds in AA5456 after UIT, around welds in AA5083 installed on-board a U.S. naval combatant and in AA5083 after *in situ* surface preparation. In the AA5456, we examined the importance of UIT parameters such as peening amplitude and pin size. It was found that all combinations of UIT parameters produced significant compressive stress but that some combinations resulted in extensive subsurface intergranular cracking in the sensitized AA5456. Optimal UIT parameters for mitigating the production of subsurface cracking were determined. In the AA5083, we examined the effect of field-based *in situ* surface preparation on residual stress measurements. The use of a portable x-ray diffractometry system to experimentally measure the distribution of residual stresses in aluminum-alloy ship structures on U.S. Navy vessels has been successfully demonstrated.

14. SUBJECT TERMS UIT, ultrasonic impact treatment, residual stress, aluminum-alloys, XRD, x-ray diffraction, AA5456, AA5083, electropolishing, metallography, sub-surface cracking, SCC, stress corrosion cracking			**15. NUMBER OF PAGES** 91
			16. PRICE CODE
17. SECURITY CLASSIFICATION OF REPORT Unclassified	**18. SECURITY CLASSIFICATION OF THIS PAGE** Unclassified	**19. SECURITY CLASSIFICATION OF ABSTRACT** Unclassified	**20. LIMITATION OF ABSTRACT** UU

NSN 7540–01–280–5500

Standard Form 298 (Rev. 2–89)
Prescribed by ANSI Std. 239–18

THIS PAGE INTENTIONALLY LEFT BLANK

SYSTEMATIC REVIEW OF ULTRASONIC IMPACT TREATMENT PARAMETERS ON RESIDUAL STRESSES OF WELDED NON-SENSITIZED VERSUS SENSITIZED ALUMINUM-MAGNESIUM

Eid Faiz Fakhouri
Lieutenant, United States Navy
B.S., Eastern Michigan University, 2006

Submitted in partial fulfillment of the
requirements for the degree of

MASTER OF SCIENCE IN MECHANICAL ENGINEERING

from the

NAVAL POSTGRADUATE SCHOOL
March 2015

Author: Eid Faiz Fakhouri

Approved by: Sarath Menon
                Thesis Advisor

                Luke N. Brewer
                Co-Advisor

                Garth Hobson
                Chair, Department of Mechanical and Aerospace Engineering

iii

THIS PAGE INTENTIONALLY LEFT BLANK

ABSTRACT

This thesis focuses on the use of x-ray diffraction to measure residual stresses around welds in 5XXX series aluminum-alloys used in naval ship structures both in the laboratory and the field. Tensile residual stresses are commonly generated during welding and, in sensitized alloys, can cause stress corrosion cracking. Peening techniques, such as ultrasonic impact treatment (UIT), can mitigate and possibly reverse these tensile residual stresses. This research uses x-ray diffraction to measure residual stresses around welds in AA5456 after UIT, around welds in AA5083 installed on-board a U.S. naval combatant and in AA5083 after *in situ* surface preparation. In the AA5456, we examined the importance of UIT parameters such as peening amplitude and pin size. It was found that all combinations of UIT parameters produced significant compressive stress, but that some combinations resulted in extensive subsurface intergranular cracking in the sensitized AA5456. Optimal UIT parameters for mitigating the production of subsurface cracking were determined. In the AA5083, we examined the effect of field-based *in situ* surface preparation on residual stress measurements. The use of a portable x-ray diffractometry system to experimentally measure the distribution of residual stresses in aluminum-alloy ship structures on U.S. Navy vessels has been successfully demonstrated.

THIS PAGE INTENTIONALLY LEFT BLANK

TABLE OF CONTENTS

THIS PAGE INTENTIONALLY LEFT BLANK

LIST OF FIGURES

THIS PAGE INTENTIONALLY LEFT BLANK

LIST OF TABLES

THIS PAGE INTENTIONALLY LEFT BLANK

LIST OF ACRONYMS AND ABBREVIATIONS

AA	aluminum-alloy
ASTM	American Society for Testing and Materials
DOS	degree of sensitization
EBSD	electron backscatter diffraction
GMAW	gas metal arc welding
GTAW	gas tungsten arc welding
MET	multiple exposure technique (residual stress measurement)
MPa	mega-Pascal
NAMLT	ASTM G67 nitric acid mass loss test
NSWCCD	Naval Surface Warfare Center Carderock Division
SET	single exposure technique (single exposure measurement)
SCC	stress corrosion cracking
SEOP	standard and emergency operating procedures
SPD	severe plastic deformation
UIT	ultrasonic impact treatment
UTS	ultimate tensile strength
wt%	weight percent
XRD	x-ray diffractometry

THIS PAGE INTENTIONALLY LEFT BLANK

ACKNOWLEDGMENTS

To my advisor, Dr. Luke Brewer, thank you for all the support and guidance throughout this research. I can emphatically say you are the most motivated professor I have ever worked for or with. Your enthusiasm for all things related to engineering materials is infectious. I wish you all the best in your career at UA and beyond.

Dr. Sarath Menon, thank you for all of your support with performing the metallography and optical microscopy of my samples. Without your guidance I would not have been able to complete my research on time.

I am grateful for financial support for this work from Mr. Richard Hays of the OSD-Corrosion Policy and Oversight Office as a part of the Technical Corrosion Collaboration Program. Also, I want to acknowledge financial support for the laboratory and field measurements from Dr. Kim Tran and Mr. Daniel Stiles of the Naval Surface Warfare Center Carderock Division. In addition, I want to express my thanks to Dr. Tran and Mr. Steve Miller of SONATS for providing the welded plates with ultrasonic treatment.

I am grateful to a number of individuals who made the field measurements on ship structures possible: Mr. Brian Wolf (NAVSEA), Mr. Bemba Dakuginow (NSWC-Carderock), Mr. Daniel Stiles, and Ms. Angela Whitfield.

I would like to thank all the professors and staff of NPS who shared their time and knowledge—in particular, Dr. Chanman Park and Mr. John Mobley, who were instrumental in assisting with laboratory setup and sample preparation, without which I could not have completed this thesis. I would also like to thank CDR Michael Porter for both his mentorship and words of wisdom. You always kept me on track and moving forward throughout my studies.

Finally, and most importantly, I want to thank my loving wife, Gada, and our three wonderful and crazy children, Zain, Danny and Yasmeen. Your smiles, hugs and kisses as I walked through the door each night always reenergized and raised my spirits. I love you all so much.

THIS PAGE INTENTIONALLY LEFT BLANK

I. INTRODUCTION

A. MOTIVATION

Following World War II, the U.S. Navy began using aluminum during construction of naval combatants in the process of building deckhouses, superstructures, or entire ships from keel to mast [1]. The primary reason for its use was to cut down the ship's weight to allow for loading more armaments. As the Navy strives to build lighter, faster, more fuel-efficient ships, the weight of structural material becomes an even greater concern. With aluminum weighing approximately one third the weight of steel, the strength benefits steel once had are becoming less significant when compared to the benefits of using lighter, marine-grade aluminum-alloys (AAs) in naval applications (see Table 1).

Table 1. Benefits of using marine-grade aluminum for naval applications, after [2].

Properties of Aluminum	Ship Result
High strength to weight ratio	Fuel Savings
Density on-third that of steel	Increased Range
Excellent corrosion resistance	Increased Payload
Weldability	Higher Speeds
Ease of forming, bending and machining	Maneuverability
High thermal and electrical conductivity	Less maintenance
Recyclable	Stability
Non-magnetic	Lower total ownership cost

Despite their many benefits in ship construction, AAs have several limitations that must be addressed, mitigated, and/or prevented to ensure a ship can remain operational for the duration of its designated service life and beyond, if possible. In particular, stress corrosion cracking (SCC) has afflicted these aluminum-based ships and is one of the major drawbacks of using AAs. When sensitized, aluminum has a substantially higher susceptibility to stress corrosion cracking than steel (see Figure 1) [3], [4]. This affects naval combatants' ability to remain a strategic national defense asset by threatening its combat survivability and requirement to meet the high, up-tempo demands. Finding innovative, low-cost solutions for mitigating stress corrosion cracking in current and future ships is a major concern for the U.S. Navy.
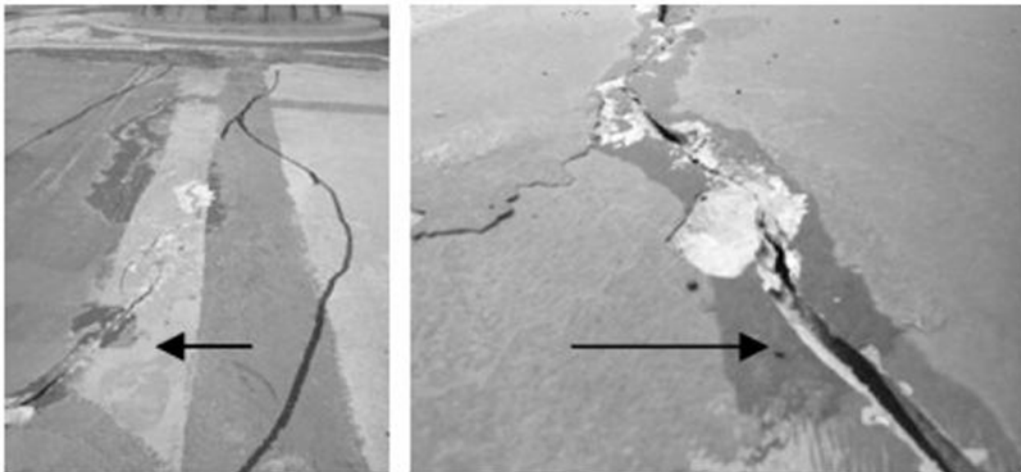
Figure 1.   Stress corrosion cracking in AA5456-H116, from [4].

The Ticonderoga class guided missile cruiser superstructure has been plagued by SCC. Maintaining this class of ship has become a primary concern for the Navy in more recent years due to new budgetary restrictions and the additional cost in developing a replacement to this aging class of ship, which is quickly approaching its service life of 35 years [4]. Currently, Congress and Pentagon officials are working to determine how maintenance planning can extend their originally designed service life. Developing a comprehensive maintenance plan for the Ticonderoga class repairs will also benefit other ship classes being built with similar AAs to include the U.S. Navy's littoral combat ship

and high-speed vessel (see Figure 2). The superstructure of the Ticonderoga class, which was built using AA5456 and has experienced extensive SCC, is the primary focus of this research.

Figure 2.   U.S. naval vessels built using marine-grade aluminum-alloy in their superstructures and/or hulls. Clockwise from top left: guided missile cruiser (CG 65), from [5]; high-speed vessel (HSV 2), from [6]; littoral combat ship (LCS 1), from [7]; and littoral combat ship (LCS 2), from [8].

Primarily, AA5456 and AA5083 are used in ship construction because of their many desired attributes, to include high strength-to-weight ratios, good as-welded strength and excellent corrosion-resistance. Although these very similar 5XXX series AAs have many positive characteristics, they also exceed 3 weight percent (wt%) magnesium, which is known to be susceptible to heat sensitization (see Table 2 and Figure 3) [9]. U.S. naval ships are commonly operating in areas of the world where local temperatures are high enough to cause sensitization over a long period of exposure.

Sensitization of 5XXX series AAs can readily begin to occur at temperatures above 60°C [10], [11]. It has even been suggested that it can become sensitized when exposed to temperatures as low as 21°C (70°F) over a long period of time (10-20 years) [9]. The sensitization process is greatly expedited at higher temperatures. These ships also operate in areas in which the ships' superstructure is continuously inundated by a corrosive seawater environment. The final of the three components required for SCC to occur is in the presence of tensile stresses generated through welding during shipbuilding, installation of new modernization upgrades and during ship repairs.

Table 2.   Weight percent of alloying elements in common aluminum-alloys used for shipbuilding. Weight percent Mg is highlighted, after [12].

	Si	Fe	Cu	Mn	Mg	Cr	Zn
AA5083	0.40	0.50	0.10	0.20-0.7	3.5-4.5	0.05-0.25	0.25
AA5456	0.25	0.40	0.10	0.5-1.0	4.7-5.4	0.05-0.20	0.25
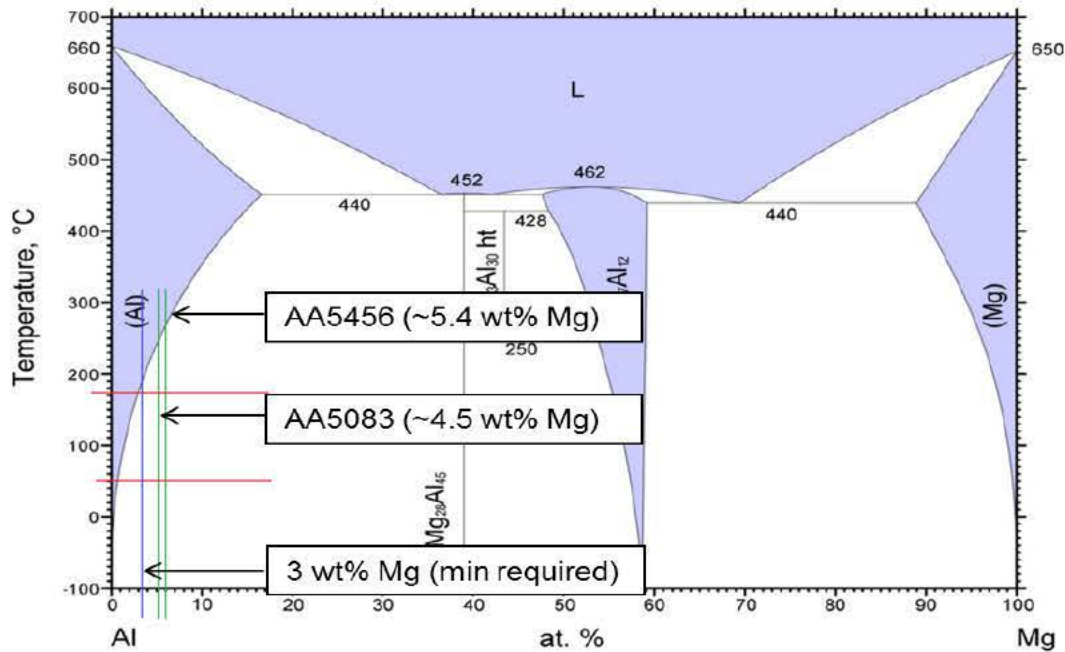
Figure 3.   Aluminum-magnesium phase diagram with 3 wt% Mg, AA5083, and AA5456 highlighted, after [13], [14].

B.   LITERATURE REVIEW

For SCC to occur in an AA, the following three conditions must be present: a susceptible material, exposure to a corrosive environment, and the presence of a tensile stress; their interdependence is represented in the Venn diagram in Figure 4. If one or more of these conditions is removed, SCC cannot occur.
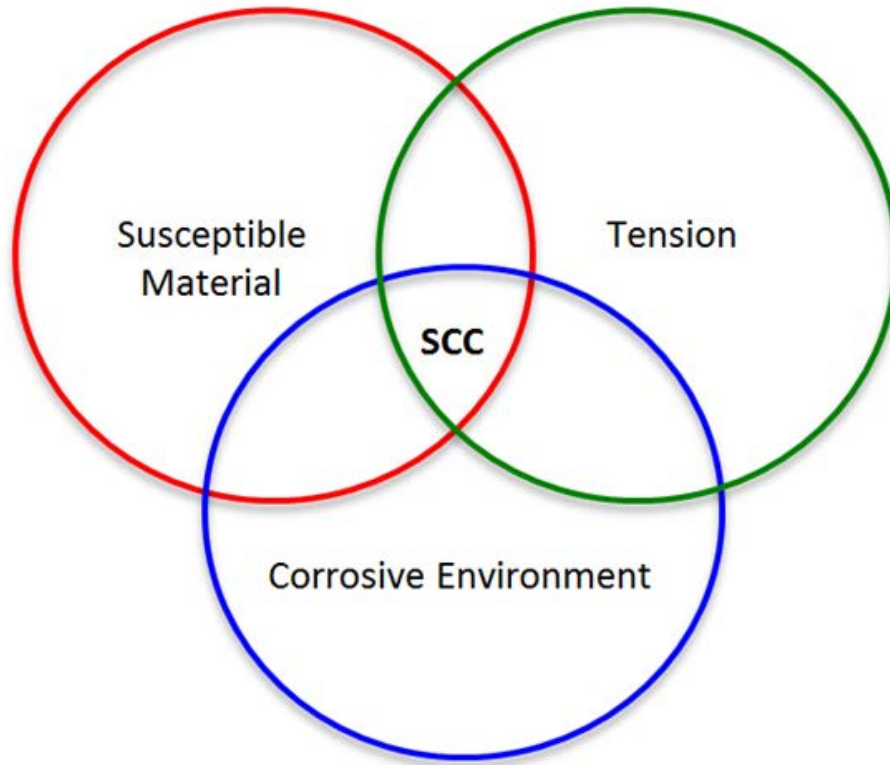
Figure 4.   Venn diagram displaying the three factors required for stress corrosion cracking (SCC).

1. SCC in 5XXX Series Aluminum-Alloys

In the case of AA5456, when it becomes sensitized, it is considered a susceptible material for SCC. Sensitization occurs as a function of both the material's magnesium (Mg) content and the amount of time it remains at an elevated temperature. The primary strengthening element used in alloying AA5456 is Mg, which, when in solid solution, increases the overall strength of the material (see Figure 5) [15]. The exposure temperature is dependent on the ship's area of operation or if welding during maintenance

or equipment modernization has occurred. When exposed to slightly elevated temperatures (>50°C) for an extended period of time (years), an aluminum–magnesium (Al–Mg) alloy with greater than 3 weight percent (wt%) magnesium will become sensitized [16]–[18]. The sensitization of the material occurs as Mg migrates out of the solid solution and forms β-phase (Al_3Mg_2) at the grain boundaries (see Figure 6). The β-phase precipitation at the grain boundaries acts as an anodic area to the Mg-depleted interior of the grain, causing a corrosive chemical reaction at the grain boundaries [16]. This causes the Al-Mg alloy's grain boundaries to be susceptible to corrosion, therefore meeting one of the three criterions for SCC.
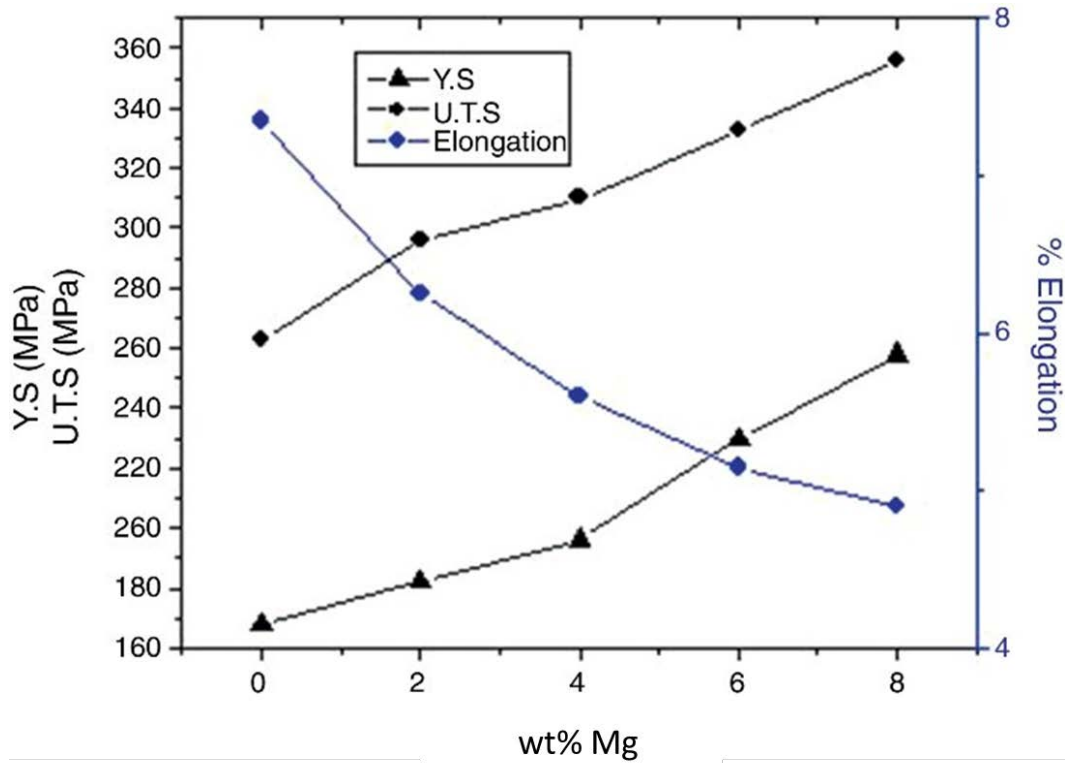
Figure 5.   Effect of magnesium in solid solution on the properties of Al–Mg alloys, from [19].
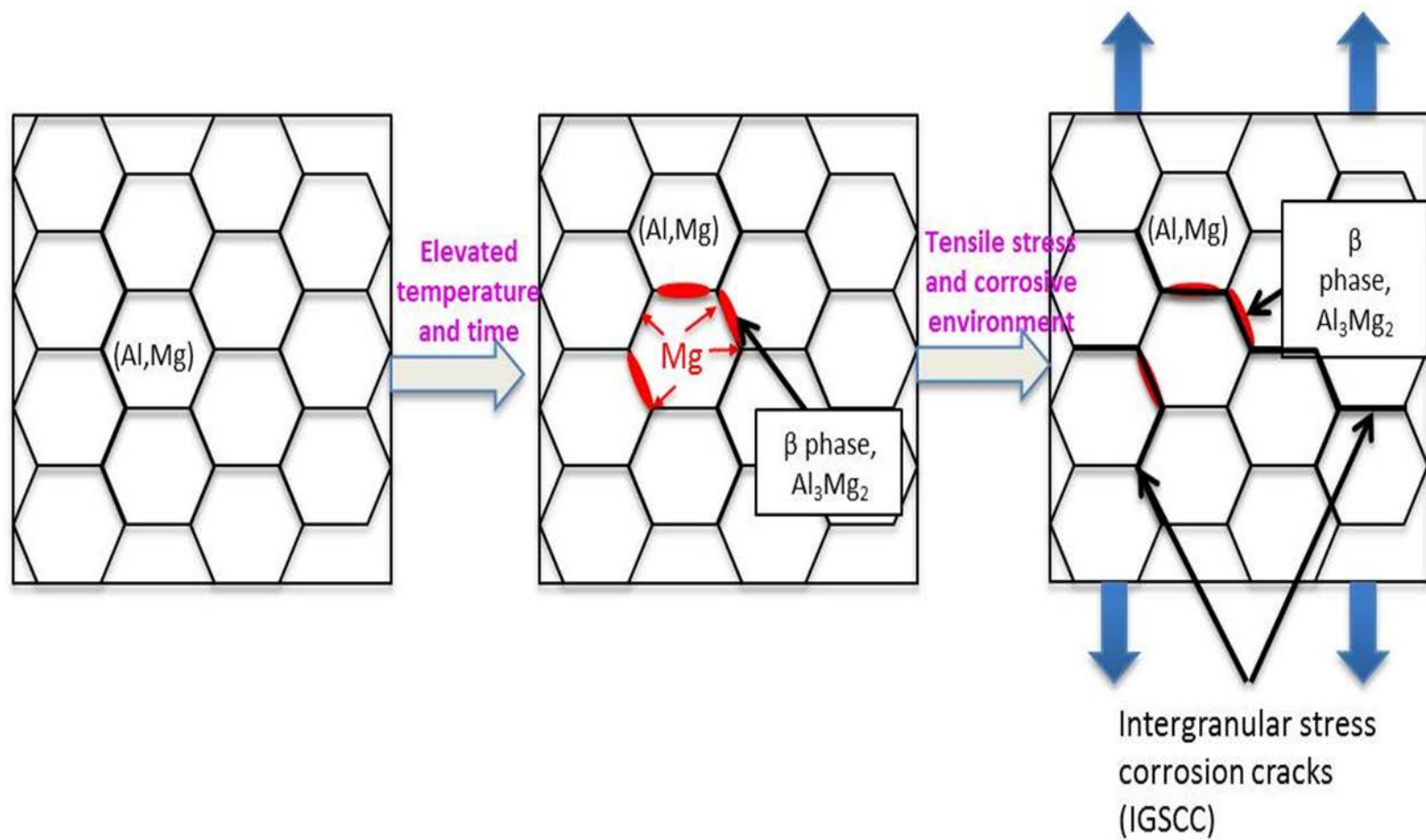
Figure 6.   Schematic illustrating sensitizations effect on a 5XXX series aluminum-alloy, from [20].

At higher temperatures, both Holtz et al. [10] and Oguocha et al. [18] found that the sensitization progression occurred much more rapidly. Holtz et al. [10] found at 175°C, AA5083-H131 began to see the effects of sensitization more rapidly (approximately at 200 hours) [10]. Similarly, Oguocha et al. [18] discovered AA5083-H116 is most susceptible to intergranular corrosion at elevated temperatures between 150 and 200°C. In a relatively short time (between approximately 10 and 200 hours) at these temperatures, magnesium atoms in the solid solution migrate to grain boundaries and precipitate into the β-phase [18].

The normal area of operation of U.S. Navy ships is in a marine environment, in which aluminum structures are exposed to a corrosive sea water environment throughout their service life. It has been shown in studies that alternating cycles of wet and dry exposure in this environment, in which concentrated amounts of chloride (dried seawater) are in contact with the aluminum, cause aggressive corrosion in aluminum structures [16], [21], [22]. Although marine-grade AAs have excellent general corrosion-resistance characteristics, this concentrated chloride environment will eventually lead to some corrosive deterioration of the material that may contribute in SCC.

Tensile stresses in a material can be characterized as either applied stresses (external) or residual stresses (internal). Applied stresses are caused by external loads supported by the material, i.e., ship loading and the weight of radars, antenna, combat weapons, and their support equipment. Residual stresses are internal to the material and are generated when a material undergoes plastic deformation (fabrication or joining of materials), large temperature gradients (welding), or during microstructural or phase transformations. The total tensile stress in a material is the combination of all the applied and residual stresses. This becomes of great concern because, in aluminum-magnesium alloys, SCC propagates at tensile stresses much lower than the materials yield strength [23].

Welding of AAs has been shown to produce significant tensile residual stresses near the welds. The large temperature gradients between the heat input and cooling rate generated during welding can leave sizeable, tensile residual stresses in the material that

may bring about SCC. Welding is used regularly on naval vessels, occurring during fabrication, construction, repairs, and installation of the new equipment. A study by James et al. [24] found residual stresses generated in gas metal arc welding (GMAW) butt welds in AA5083 reached tensile stresses near 100 MPa at approximately 20 mm from the toe of the weld (see Figure 7) [25]. The magnitude of tensile stresses produced during welding are the product of many factors, to include geometry, orientation, and linear heat input of the weld [15]. When sensitized 5XXX series AAs are welded, these tensile stresses, in combination with a corrosive marine environment, may drive stress corrosion cracking (see Figure 6).
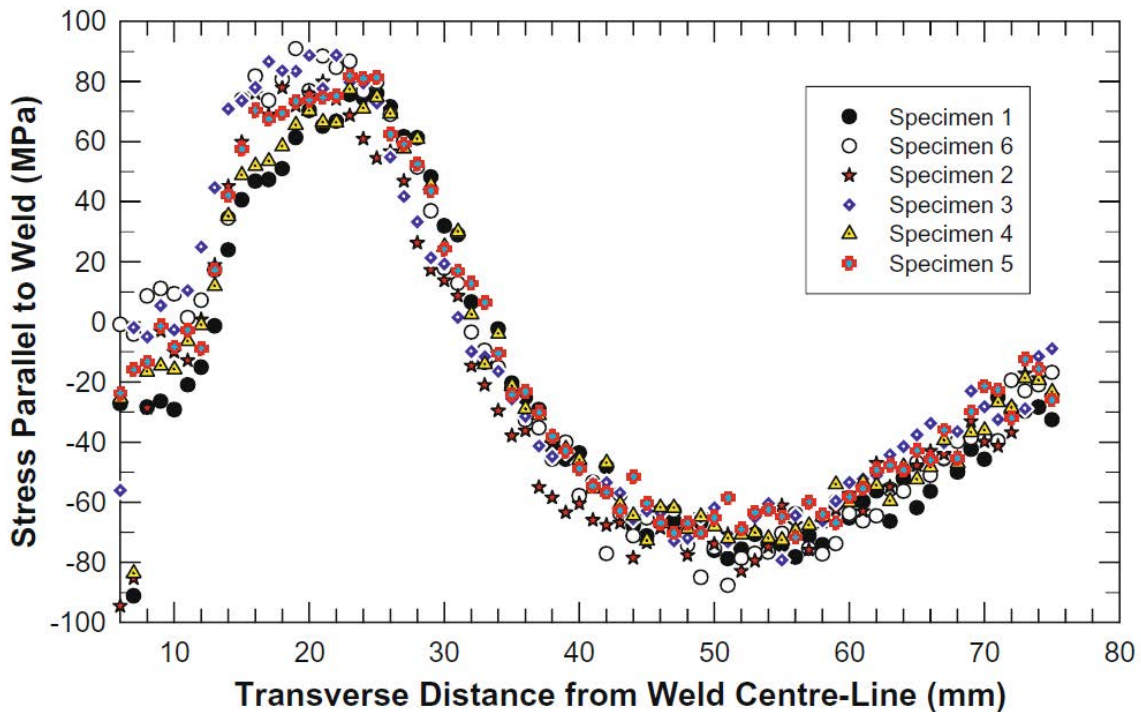
Figure 7.   Residual stress data parallel to the weld in as-welded state of GMAW butt welds in AA5083. Measurements were conducted using synchrotron x-ray diffraction, from [25].

2. Ultrasonic Impact Treatment

Tensile residual stresses can be mitigated in part by the use of peening techniques on the surfaces of welded aluminum components. Ultrasonic impact treatment (UIT) is a peening technique which uses a small diameter pin, or set of pins, vibrating at ultrasonic frequencies to plastically deform the surface of a material. Along with UIT, other peening techniques, such as shot or laser peening, are essentially cold working processes that change a material's properties by plastic deformation of the material's surface. The plastic surface deformation removes tensile stresses by induction of compressive stresses. This in turn improves material properties such as corrosion fatigue and fatigue resistance. Zoeller et al. [26] found that shot peening AAs can form residual compressive stresses improving fatigue life. Their study has shown that shot peening aided in preventing widespread SCC of AAs used in aircraft and suggests continued use will reduce future SCC failures [27].

Although most peening processes produce the same results, UIT holds an advantage over others due to its cost effectiveness and ease of portability [28], [29]. Most UIT devices are hand held, have very few moving parts, require little to no surface preparation and do not produce any residual material necessitating clean-up. Its portability is especially useful on ships where tight spaces and awkward weld geometries are common place [30].

The SONATS hand held UIT devices, pictured in Figure 8 and Figure 9; create ultrasonic frequencies that are converted to a mechanical displacement of its pin by its piezo-electric emitter. The signal is amplified through various signal promoters before the mechanical vibration is finally transferred to the peening needles (pins). No additional force is required to be applied by the operator, they only need to guide the hand held applicator over the desired region. The pin diameters used can be varied but in shipboard applications is usually 1, 3, or 4 mm in diameter. The vibration amplitude of this device ranges from 10 to 250 μm, and is occasionally designated by percent of input power [31]. Different combinations of the two UIT parameters of vibration frequency (percent input power) and pin size can be selected to produce a range of surface treatments.
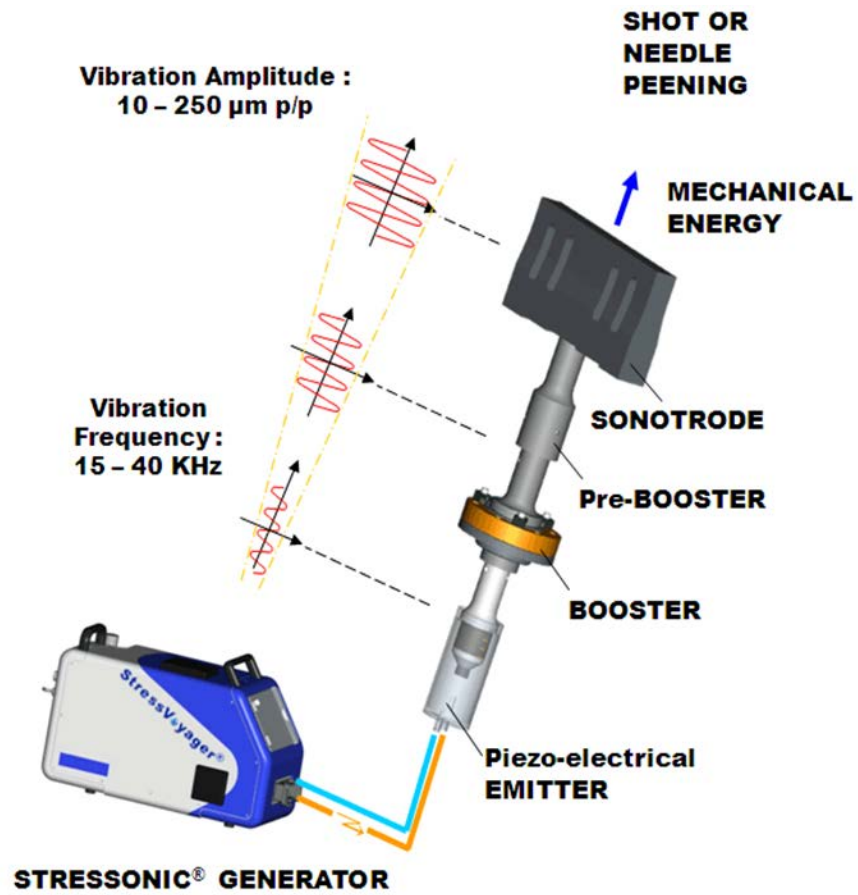
Figure 8.   General schematic of a SONATS UIT device with a multi-pin applicator attached, from [31].

Figure 9.   Portable SONATS UIT device with a single-pin applicator attached, from [32].

UIT is effective at placing compressive stresses on the surfaces of aluminum components. UIT eliminates residual tensile stress generated during welding by inducing compresses stresses greater than -150 MPa in most AAs and approximately -500 MPa in steels [28], [33], [34]. The depth to which UIT induced compressive stress can vary greatly depending on the specific material characteristics and instrument parameters used. A study by Liao et al. [35] compared before and after UIT results as a function of depth in AA7075-T651, used primarily for aircraft structural components, found compressive stresses present up to an evaluated depth of 1 mm (see Figure 10). Goudar et al. [33] supports these findings, reporting compressive stresses at depths in excess of 2–4 mm in thicker steel plates. Multiple studies show that removal of tensile stresses by generating compressive stresses will substantially increase a material's ability to resist corrosion and wear, and can improve its fatigue life [27], [28], [34]–[39].
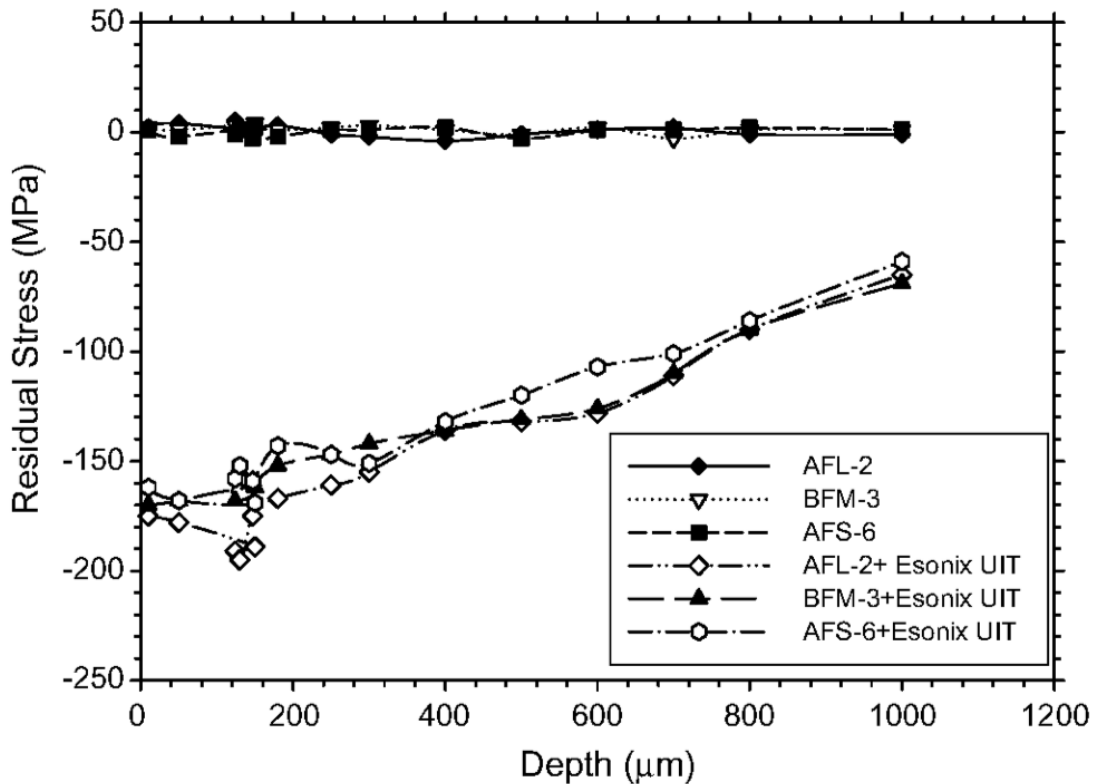
Figure 10.   Residual stress distribution prior to and after UIT on 7075-T6511 aluminum specimens, from [35].

12

The severe plastic deformation of the materials surface during UIT may cause surface and subsurface microstructural damage. A study of the microstructural evolution of severely plastically deformed, sensitized AA5456 by Tran et al. [36] found micro voids, tears, and the formation of a delamination layer between UIT surface and metal below. The research by Castillo-Morales et al. [34] suggest that, at specific UIT parameters of impact frequency, load amplitude, pin size diameter, etc., adequate compressive stresses will be generated preventing microstructural subsurface cracking or tearing to occur in AA2024-T3. Although this and other studies on the effects of UIT on aluminums and steels have yielded a wealth of knowledge on the topic, none were dedicated to the systematic study of various UIT parameters' effects on the materials microstructure and residual stress level.

3. X-Ray Diffraction Measurements

The residual stresses generated by both welding and by peening methods, such as UIT, can be measured by either destructive (e.g., hole-drilling, slit-compliance, contour method etc.) or non-destructive (e.g., laboratory x-ray, synchrotron x-ray, neutron diffraction, etc.) methods. X-ray and neutron diffraction have both been used to measure residual stress distributions in aluminum welds [40]. In particular, James et al. [25] have used synchrotron x-ray diffraction to measure the residual stress distribution in GMAW welds of AA5083. They observed tensile stresses as high as 100 MPa parallel to the weld. While synchrotron x-ray and neutron diffraction are able to measure three-dimensional distributions of residual stress through thick (10-30 mm thick) aluminum structures, they require large, special purpose facilities that cannot be used on a routine basis or to perform field measurements. Laboratory x-ray diffraction has also been successfully implemented to measure the residual stresses on the surface of aluminum welds before and after UIT [37]. This same type of x-ray diffraction residual stress measurement has also been made portable and has recently been used to measure residual stresses on a Canadian submarine [41].

X-ray residual stress measurements are based upon the measurement of elastic strain in the atomic lattice of crystalline materials. The stress is calculated from the

measured strains using linear elasticity theory and known materials elastic constants. The strain is measured as the stress-induced shift in the spacing between planes of atoms in the crystalline lattice. This "d-spacing," d_{hkl}, can be related to the x-ray diffraction angle through Bragg's law (Equation 1).

$$d_{\varphi\psi} = \frac{\lambda}{2\sin\theta} \qquad\qquad \text{Equation 1}$$

Lambda (λ) is the wavelength of the incident x-rays and theta (θ) is the Bragg diffraction angle.

The geometry of the x-ray diffraction-based residual stress experiment is based upon the Bragg-Brentano circle (see Figure 11). The lattice spacing, $d_{\phi\psi}$, is the measurement of the lattice spacing for a given {hkl} reflection at a given sample orientation (ϕ) and a given x-ray source orientation (ψ). The strain component perpendicular to the scattering vector, Q, is given by Equation 2.

$$(\varepsilon'_{33})_{\varphi\psi} = \frac{d_{\varphi\psi} - d_o}{d_o} \qquad\qquad \text{Equation 2}$$

The unstrained lattice spacing (d_o) is determined from measurements taken normal to the material's surface. By measuring a series of ε'_{33} values at different ψ angles, the strain components ε_{ij} can be determined for a given sample orientation, ϕ, by solving the following system of equations:

$$\left(\varepsilon'_{33}\right)_{\phi\psi} = \frac{d_{\phi\psi} - d_0}{d_0} = \varepsilon_{11}\cos^2\phi\sin^2\psi + \varepsilon_{12}\sin 2\phi\sin^2\psi + \varepsilon_{22}\sin^2\phi\sin^2\psi$$

$$+ \varepsilon_{33}\cos^2\psi + \varepsilon_{13}\cos\phi\sin 2\psi + \varepsilon_{23}\sin\phi\sin 2\psi \qquad \text{Equation 3}$$

Typically, ε_{13} and ε_{23} are assumed to be close to zero, thus Equation 4 becomes:

$$\left(\varepsilon'_{33}\right)_{\phi\psi} = \varepsilon_{11}\cos^2\phi\sin^2\psi + \varepsilon_{12}\sin 2\phi\sin^2\psi + \varepsilon_{22}\sin^2\phi\sin^2\psi + \varepsilon_{33}\cos^2\psi$$

$$\text{Equation 4}$$

Equation 5 is linear when plotted against the value $\sin^2\psi$. If one assumes isotropic elastic properties and that the stress normal to the sample surface, σ_{33}, is zero (assumed in x-ray diffraction because x-rays do not penetrate more than a few tens of microns) [42]. The measured strain can be related to the stress as:

$$\left(\varepsilon'_{33}\right)_{\phi\psi} = \frac{1+\nu}{E}\left\{\sigma_{11}\cos^2\phi + \sigma_{12}\sin 2\phi + \sigma_{22}\sin^2\phi\right\}\sin^2\psi - \frac{\nu}{E}\left(\sigma_{11} + \sigma_{22}\right)$$

$$\text{Equation 5}$$

At $\phi=0$, the level of stress is simply the linear slope of ε'_{33} plotted against $\sin^2\psi$. This behavior is termed "regular" $\sin^2$ behavior and is the basis for traditional laboratory x-ray residual stress measurements [43]. The components of σ_{11}, σ_{22}, and σ_{12} can be measured independently by repeating this measurement for different values of the sample orientation, ϕ.
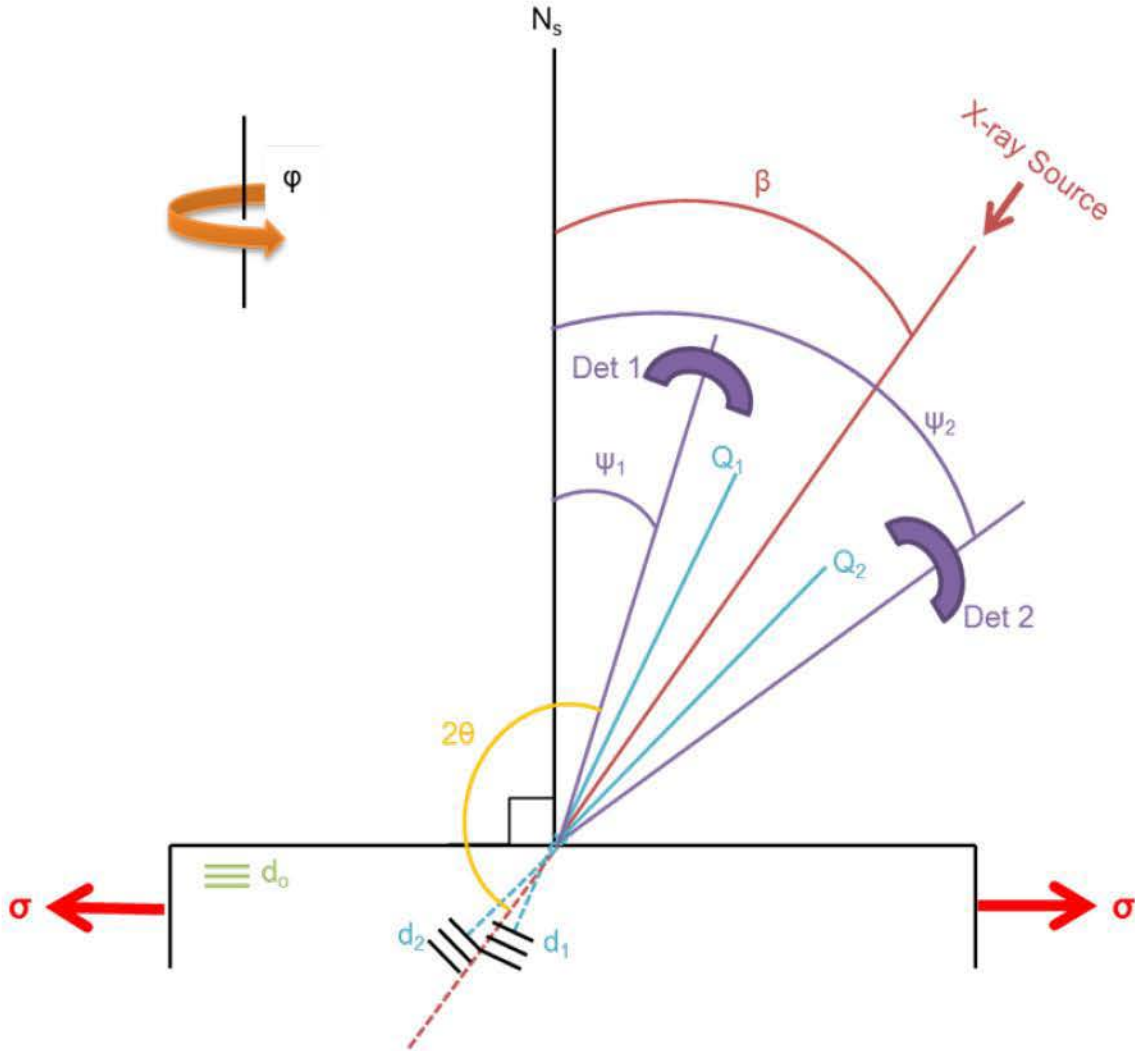
Figure 11. Schematic of x-ray diffraction geometry for residual stresses measurement in a crystalline material, from [13].

C. THESIS OBJECTIVES

This thesis focuses on the use of x-ray diffraction to measure residual stresses around welds in 5XXX series AAs used in ship structures both in the laboratory and the field. This research uses x-ray diffraction to measure residual stresses around welds in AA5456 after UIT, around welds in AA5083 installed onboard a U.S. naval combatant and in AA5083 after *in situ* surface preparation.

The following objectives were established for research in this thesis:

1. Assess the importance of UIT conditions, such as amplitude and pin diameter, on the level of elastic stress and plastic strain generated in welded and treated AA5456.

2. Determine the role of sensitization in the generation of residual stresses and in the evolution of microstructure after UIT.

3. Perform x-ray residual stresses on welded aluminum-alloy structures on a U.S. naval vessel.

II. EXPERIMENTAL METHODS

X-ray residual stress measurements were taken on welded aluminum-alloy (AA) 5456 (Al-5.1Mg-0.8Mn-0.12Cr) plates using x-ray diffraction (XRD). The analysis of AA5456 plates in this thesis is a continuation of previous thesis work conducted by LT Michelle Haggett, United States Navy [13]. Measurements were performed using the same testing methods to ensure continuity and consistency of collected data for results comparison. The plates were both sensitized and non-sensitized, joined by gas metal arc welding (GMAW), and then surface treated using ultrasonic impact treatment (UIT). Optical microstructural analysis was conducted on samples from both AA5456 non-sensitized and sensitized GMAW joined UIT treated plates. XRD was also used to measure residual stresses of a non-sensitized plate of AA5083 (Al-4.4Mg-0.7Mn-0.15Cr) with multiple *in situ* surface preparations performed. The non-sensitized AA5456 plates were provided by Naval Surface Warfare Center Carderock Division (NSWCCD). The sensitized AA5456 plates were cut from the superstructure of a U.S. Navy Guided Missile Cruiser. Electrolytic polishing was conducted on two areas of non-sensitized AA5456 plates and on two locations of the non-sensitized AA5083. Field-based residual stress measurements were taken of AA5083 installed on-board a U.S. Navy ship.

A. LABORATORY EXPERIMENTS

1. Systematically Ultrasonic Impact Treated, Gas Metal Arc Welded, Aluminum-Alloy 5456 Plates

The sensitized aluminum plates were comprised of two 37 cm (14.6 in) wide, 36 cm (14.2 in) long, and 6.35 mm (0.25 in) plates cut from the superstructure of a U.S. Navy Guided Missile Cruiser (see Figure 12 and Table 3). ASTM G67 testing for degree of sensitization (DOS) was performed on the aluminum and indicated DOS levels which ranged from 40 to >60 mg/cm^2. The non-sensitized plates consisted of two 35.6 cm (14 in) wide, 51 cm (20 in) long, and 9 mm (0.35 in) thick, non-sensitized AA5456 (see Figure 13 and Table 3). The plates were butt welded parallel to the rolling direction using a 60 degree double-v-groove configuration with an AA5556 filler metal. A single weld pass was performed on each side. This configuration helped reduce distortion and

17

residual stresses incurred during welding. Welding parameters were similar for both the sensitized and non-sensitized plates with the exception of the shielding gas. A 100 percent He-gas was used for the non-sensitized plates vice the 75/25 percent He/Ar mixture used when welding the sensitized plates (see Table 4). DOS testing and welding were performed by NSWCCD.

Figure 12.   Sensitized, GMAW butt welded AA5456-H116 at various UIT conditions. Clockwise from top left: Surface A, C, D, and B.

18
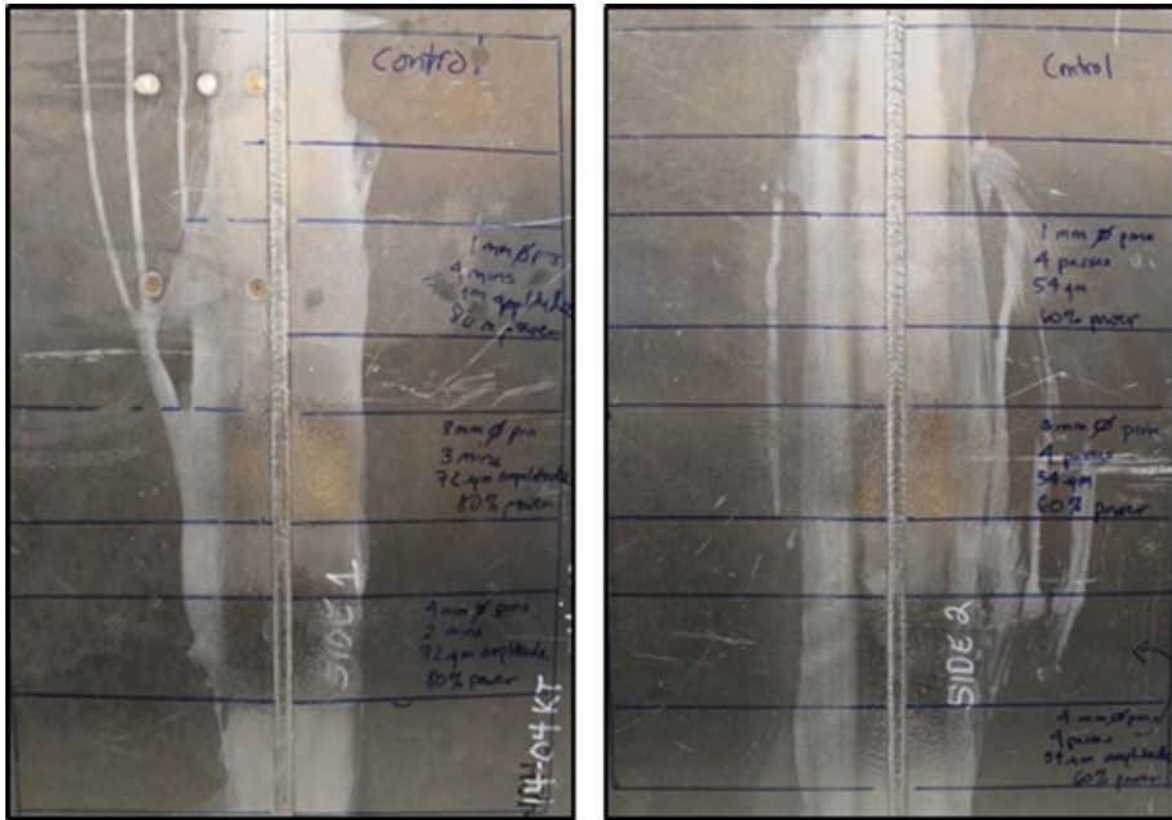
Figure 13.   Non-sensitized, GMAW butt welded AA5456-H116 at several UIT
conditions. Left: Surface A. Right: Surface B.

Table 3.   Ultrasonic impact treatment parameters conducted on AA5456-
H116 plates by Empowering Technologies (SONATS).[1]

	Weld Surface	Power (%)	Amplitude (μm)	# Passes	Amplitude (μm)	# Passes
			Sensitized AA5456		Non-Sensitized AA5456	
Surface A	Crown	80	51	4	72	*
Surface B	Root	60	38	4	54	4
Surface C	Crown	40	25	3	36	3
Surface D	Root	20	12	4	18	4

[1] The power level corresponded to displacement amplitude of the pin.

* For Surface A of the non-sensitized AA5456 plate, UIT was measured in length of treatment time vice number of passes (4min@1mm pin, 3min@2mm pin, and 2min@1mm pin).

Table 4.   NSWCCD GMAW parameters used when welding the AA5456-H116 plates.

	Sensitized AA5456	Non-Sensitized AA5456
Process	GMAW-P	GMAW-P
Base Metal	5456-H116	5456-H116
Filler Metal	5556 (3/64 inch diameter)	5556 (3/64 inch diameter)
Current (Amps)	85-90	85-90
Voltage (V)	24.7	24.7
Shielding Gas	75/25 He/Ar	100 He

The UIT on the plates was completed by Empowering Technologies a subsidiary of SONATS. Each surface (A, B, C, and D) of the sample set two was divided into four distinct zones (see Table 3). Each zone received a UIT treatment with a different combination of pin size and power level. One zone on each surface was designated as the "Control," and no UIT was performed in that zone. The different zones were clearly marked and equally distributed on the plate. The UIT region of each zone went out in both directions approximately 100 mm (approximately 4 inches) from the center of the weld. The remaining three zones of each surface had a specified power input and pin diameter size (see Figure 14).
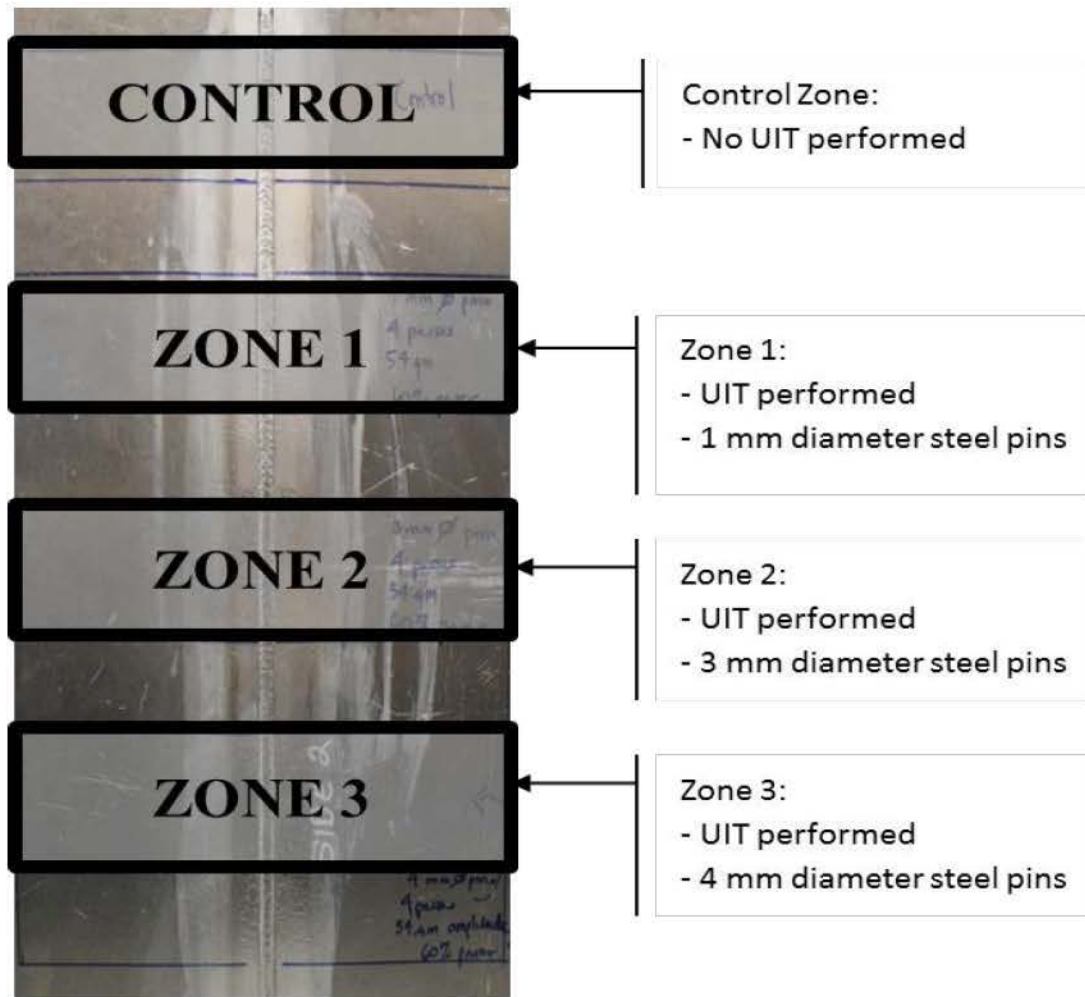
Figure 14.   Photograph of UIT geometry performed in each zone for each
AA5456 plate.

2. Residual Stress Measurements

The Proto iXRD Residual Stress Analyzer was used to measure the residual stresses of each sample area tested in this thesis. The analyzer's primary function is to perform residual stress measurements by x-ray diffraction. During laboratory measurements the analyzer was operated within the manufacturer's radiation safety enclosure. When operated during field-based measurements an open-beam configuration was used. All measurements, whether in lab or field-based, were in accordance with NPS Open-Beam Standard and Emergency Operating Procedures (SEOP) [44] and U.S. Navy radiation safety requirements [45].

Proto equipment startup and warmup was completed daily in accordance with Proto and NPS SEOP [44], [46]. Alignment of detectors was verified prior to collecting data by using stress-free powder and high-stress aluminum standards. The 99.5 percent pure aluminum stress-free powder standard was leveled and centered beneath the analyzer collimator (see Figure 15). The autofocus function of the analyzer was used to determine the proper "Z" position of the collimator and detectors for each measurement. Upon completion of autofocus verification a 2 mm aperture was placed in the collimator and used for each measurement. A diffraction profile was taken of the stress-free powder sample with the beta and phi angles set to zero (see Figure 16).
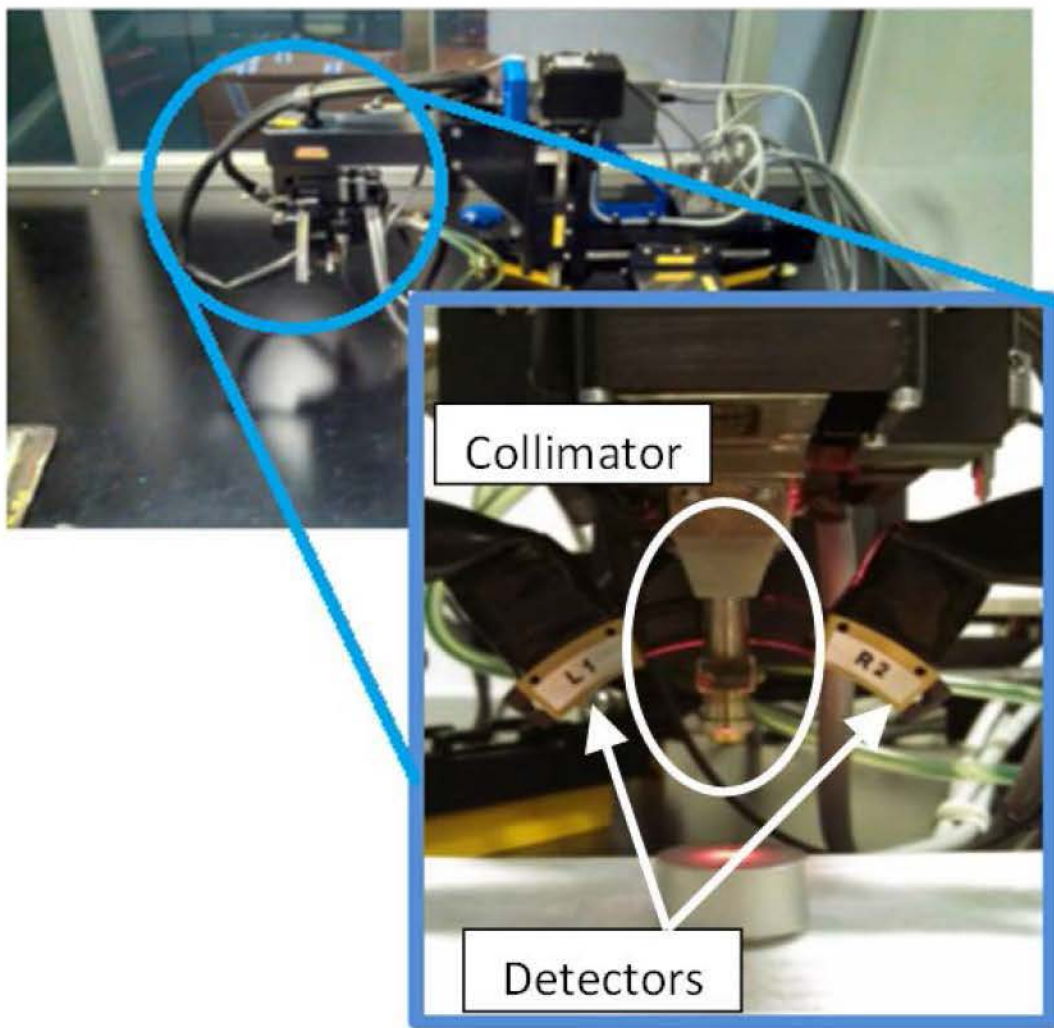
Figure 15.   The Proto manufacturing iXRD with close-up of collimator used to collect residual stress values for AA5456 samples.
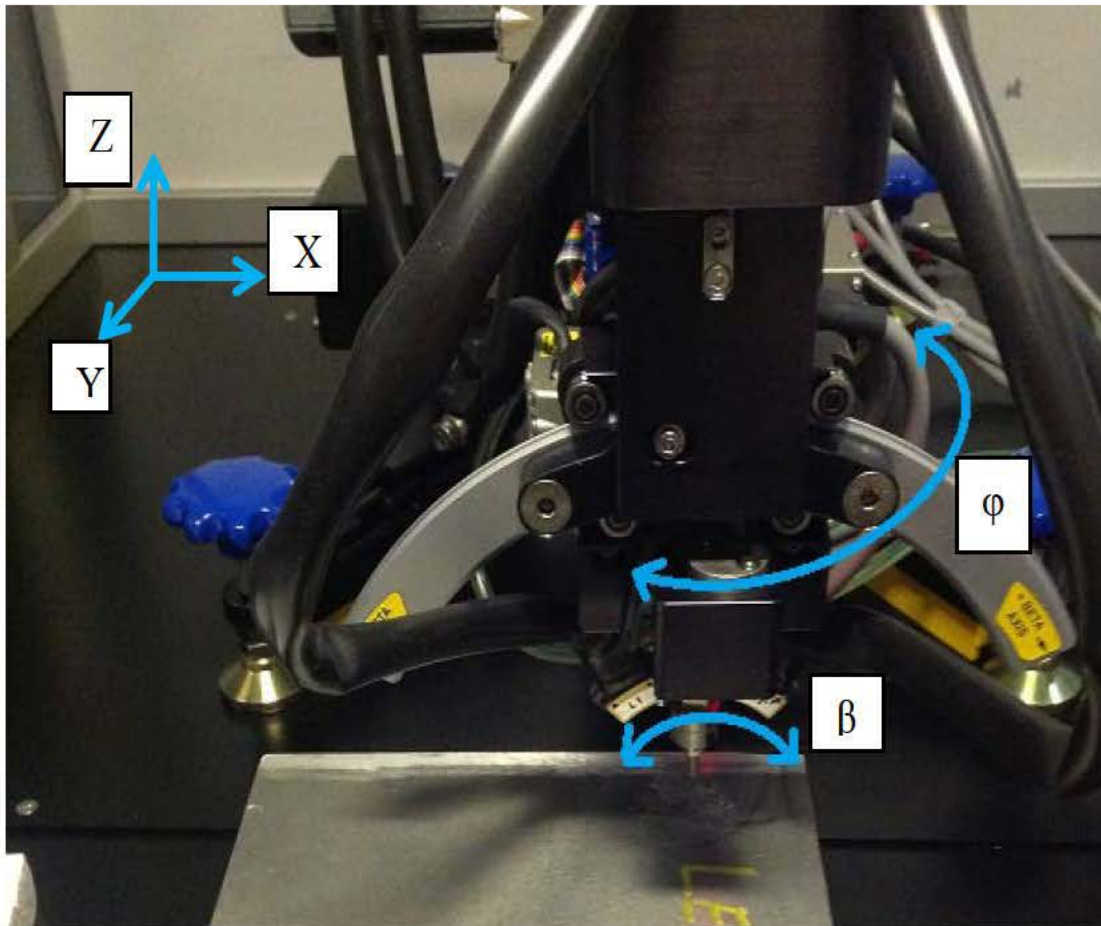
Figure 16.   The Proto Manufacturing iXRD with each axis labeled. The X, Y and Z axis had a range of ±50 mm from the zero position. The β axis had an arc from ±45°. The φ axis had a range of 0° to 180°.

Detector placement was determined by ensuring the diffraction peak was centered and that the selected region of interest was large enough to allow peak broadening while also preventing interference from any possible secondary peaks (see Figure 17). A single exposure measurement of a β-titanium shim was taken to establish a background signal level that was subtracted during the diffraction peak analysis of the remainder of measurements (see Figure 18).
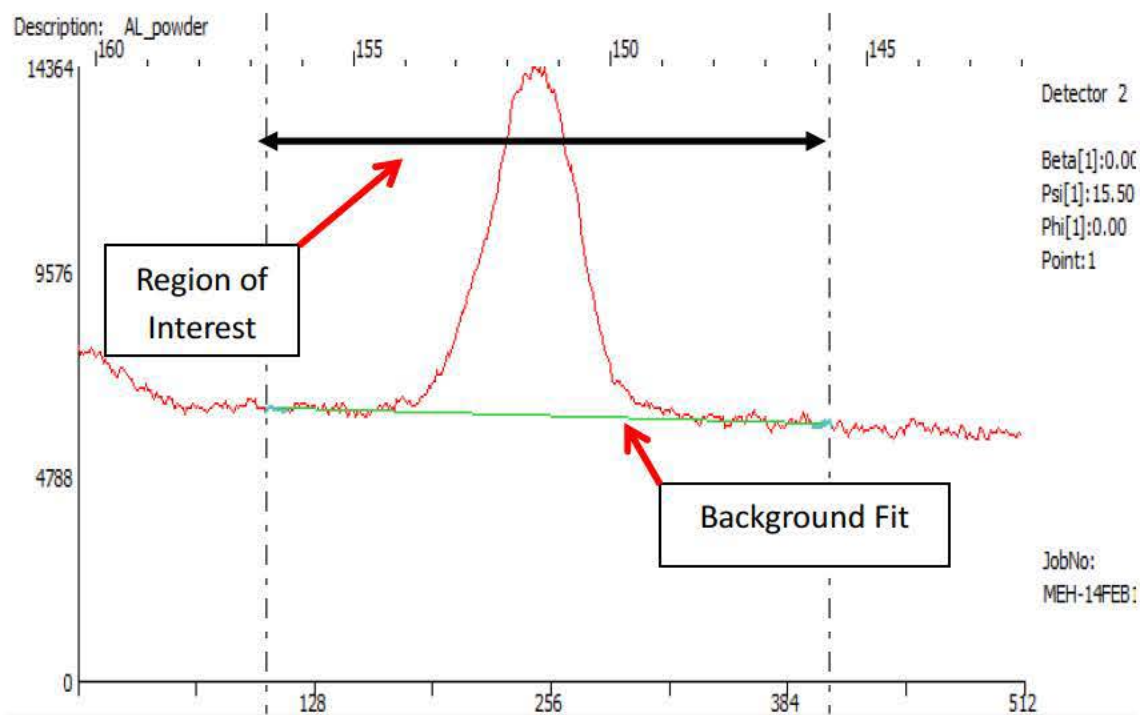
Figure 17.   Results from a single exposure measurement profile of the stress-free aluminum powder standard.
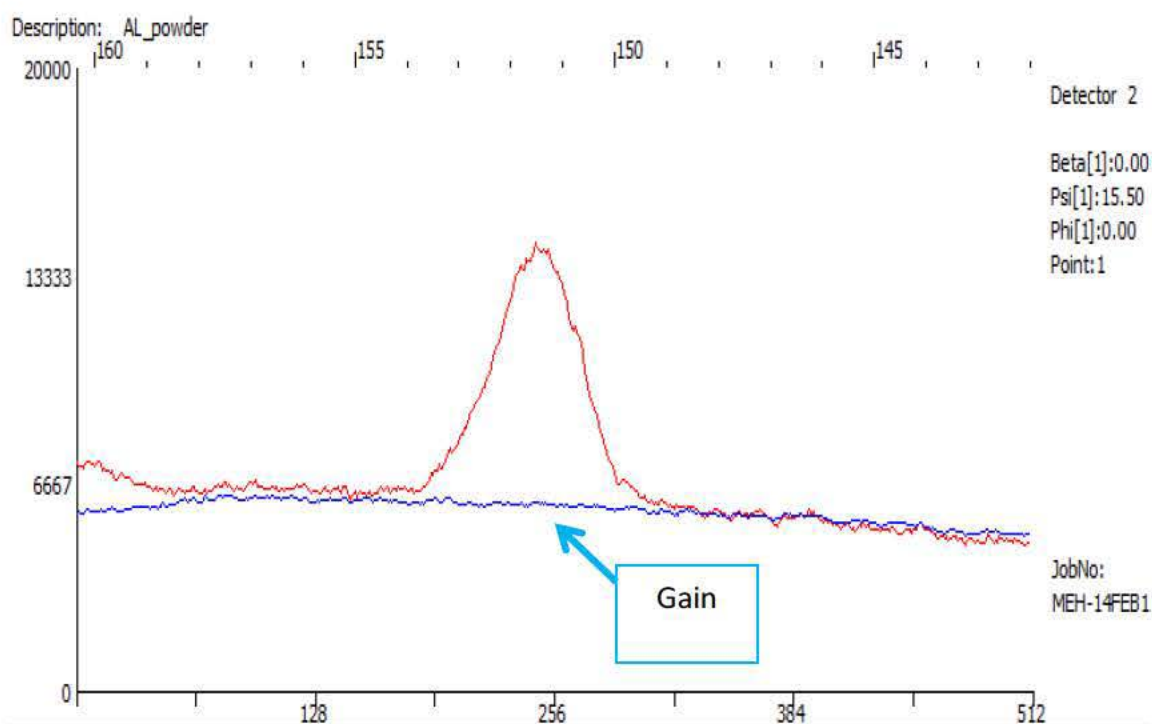
Figure 18.   Line profile of a single exposure measurement taken on the stress-free aluminum powder standard.

A residual stress measurement from a single point required the collection of multiple diffraction profiles at a series of beta (incidence) angles. A residual stress measurement of the stress-free aluminum standard powder was collected with the phi angle set to zero and the beta angles evenly distributed from -25 to 25 degrees. Diffraction peaks at each of the eleven, beta angles were analyzed to check for irregularities (see Figure 19). Although there was little, if any, shift in the diffraction peak, the region of interest and background fit were manually adjusted to ensure the diffraction peaks from each of the beta angles were included. Once acceptable data from the stress-free standard residual stress measurements were taken a residual stress measurement of the high-stress standard was then taken using the same measurement parameters for previous measurements (see Table 5).
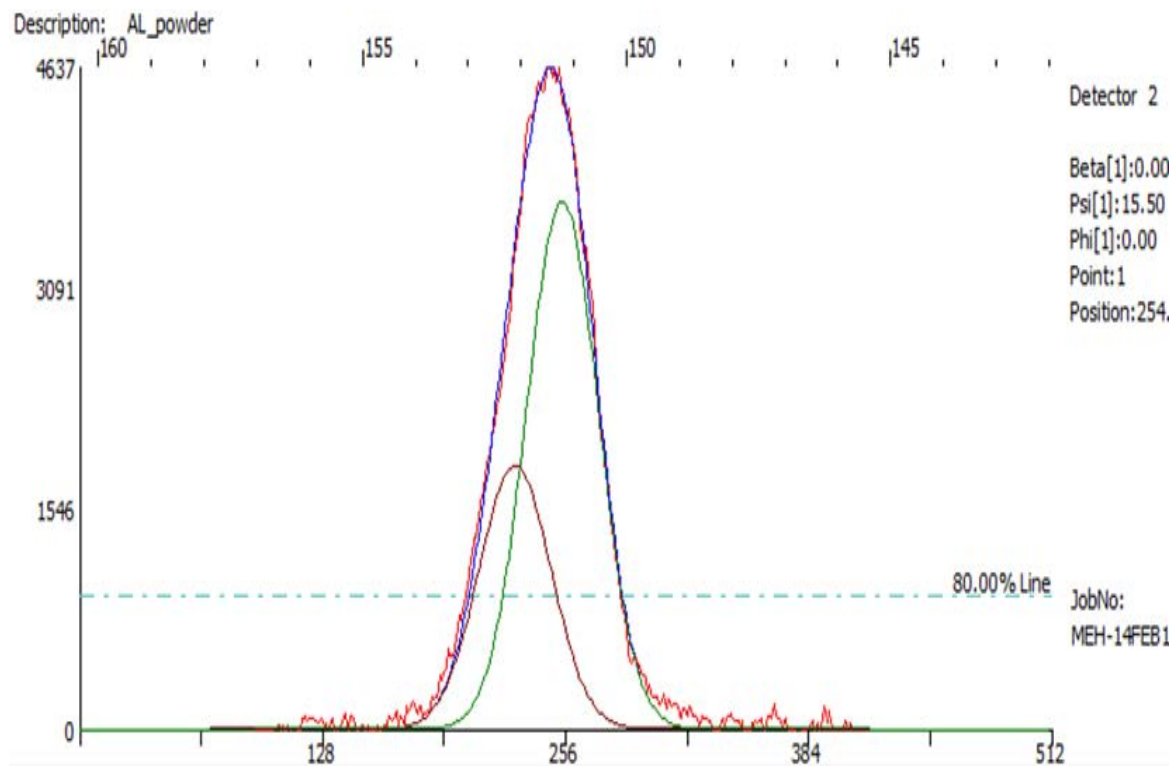
Figure 19.   Line profile of one of eleven beta angles taken during a residual stress measurement on the stress-free aluminum powder standard.

25

Table 5.   Proto iXRD parameters for laboratory-based residual stress measurements on AA5456-H116.

Tube Radiation Type	Cobalt K-alpha
Location of Detectors	Outside edge of knob at ~143 on arc
Data Collection Parameters	20kV, 4mA
Gain Parameters	10kV, 4mA
Aperture	2mm diameter
Beta Angle	11 total evenly spaced from 25 to -25 degrees
Exposures	5
Exposure Time	5 seconds
Exposure Gain	40
Miller Index	{331} Reflection
Bragg Angle	149 degrees
Gain Shim	Beta Titanium

The d-spacing versus $\sin^2\psi$ graphs produced during the residual stress measurement for both the stress-free and high-stress aluminum standard were used to verify alignment of the system. For the stress-free powder sample a measured residual stress of 14 MPa out-of-plane sheer stresses was required to verify alignment. The aluminum high-stress standard contained a known compressive stress of 274 MPa. As shown in Figure 20, the d-spacing versus $\sin^2\psi$ has a negative slope and minimal branch splitting. Examples of recorded alignment verification data compared to the aluminum stress-free and high-stress standard allowable limits are listed in Table 6.
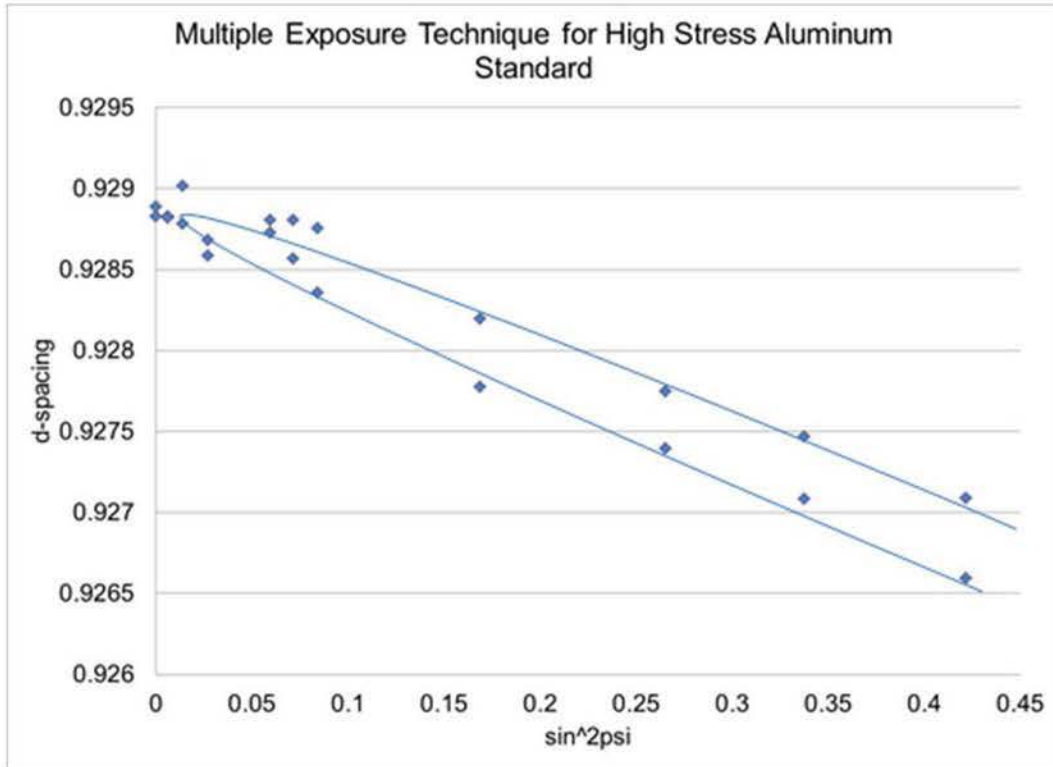
Figure 20. D-spacing versus $\sin^2\psi$ results from a multiple exposure technique measurement on the high-stress aluminum standard.

Table 6. Acceptable values of stress measurements collected for aluminum powder and high-stress standards.

Acceptable Value for Aluminum Powder Standard	Acceptable Value for Aluminum High-Stress Standard
$\sigma=0 \pm 14$ MPa $\tau= 0 \pm 10$ MPa	$\sigma=-274 \pm 23$ MPa $\tau= 0 \pm 10$ MPa
Example of Values Achieved	**Example of Values Achieved**
$\sigma=-5.2 \pm 2.1$ MPa $\tau=-2.2 \pm 0.9$ MPa $\sigma=-3.0 \pm 1.7$ MPa $\tau=-2.7 \pm 0.8$ MPa $\sigma=-8.16 \pm 4.35$ MPa $\tau=-4.9 \pm 2.1$ MPa	$\sigma=-276.3 \pm 8.4$ MPa $\tau=-1.4 \pm 3.7$ MPa $\sigma=-282.8 \pm 6.5$ MPa $\tau=4.4 \pm 3.6$ MPa $\sigma=-267.8 \pm 10$ MPa $\tau=-5.1 \pm 3.9$ MPa

3. Electrolytic Polishing

The Proto Electrolytic Polisher Model 8818-V3 was used to remove layers of surface material from specified areas of the aluminum samples to allow for depth-resolved residual stress measurements (see Figure 21). A 10 percent perchloric acid-90 percent ethanol solution chilled in a freezer to approximately 0 degrees Celsius (32 degrees Fahrenheit) with an applied voltage of 20 volts was used. The solution was chilled to increase its viscosity and aid in removal of surface material. These parameters resulted in a current between 0.1-0.2 amperes and a material removal rate between 500–1000 μm per 5 minutes of run-time. A 15 mm (0.6 in) diameter rubber applicator tip was used on the probe producing circular polished area with a diameter of approximately 12 mm (0.5 in) (see Figure 21 and Figure 22). To maintain viscosity of the solution was chilled in a freezer between applications. Depth measurements were taken using the Proto XRD automatic positioner.

Figure 21.   Proto Electrolytic Polisher Model 8818-V3 used to remove surface material for depth-resolved measurements.
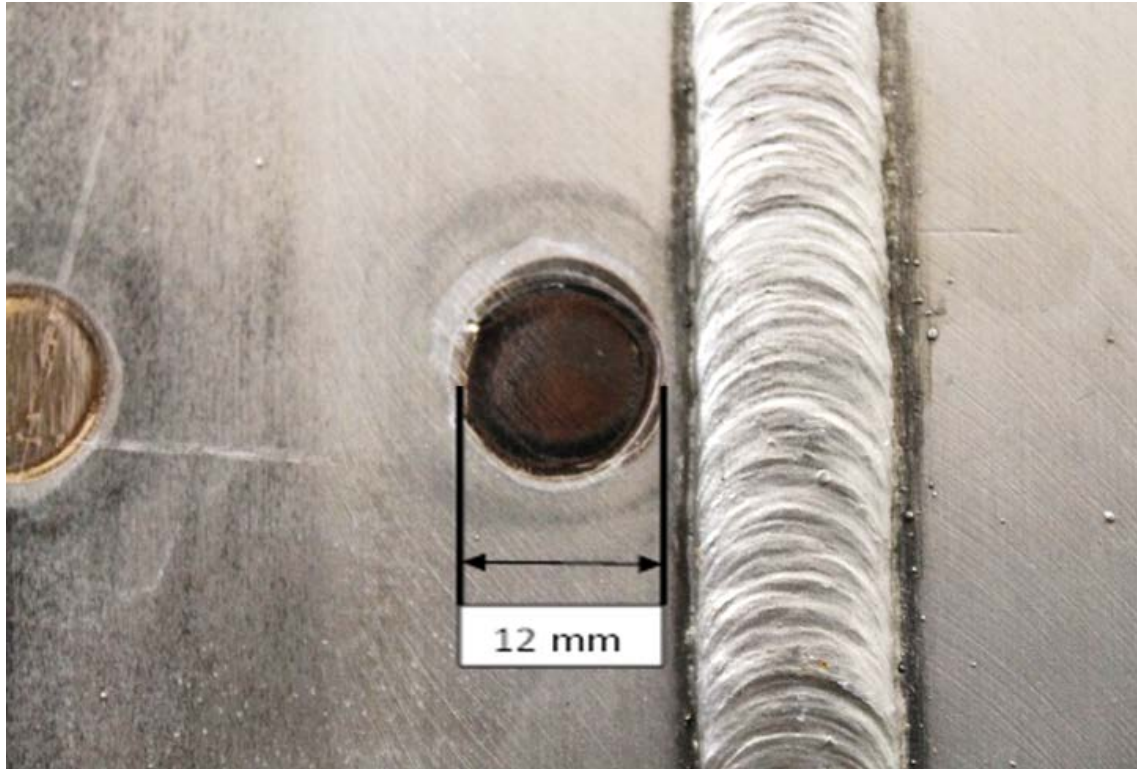
Figure 22.   The figure shows an electropolished area of an AA5456 plate
produced using a Proto Electrolytic Polisher with a 15mm adaptor tip
and a 10 percent perchloric–90 percent ethanol solution.

4. Optical Microscopy

Optical microscopy was used to examine the microstructure of the aluminum after UIT. Cross-sectional samples were cut transverse to the weld from each zone of sample sets one and two; a total of 12 samples, each approximately 6 millimeters (.24 inches) wide and 15 millimeters (.59 inches) long. Each sample was then individually mounted in epoxy molds to allow for metallographic polishing of the cross-section of the weld (see Figure 23). This configuration was used to examine the microstructure as a function of depth from the weld toe through the HAZ and beyond.

Figure 23.   Samples of AA5456 mounted in epoxy molds prior to performing metallographic polishing.

The samples were polished using a Buehler Automatic Variable Speed Grinder-Polisher Model ECOMET 4. Standard metallography techniques were used, systematically stepping down from 1200 grit silicon-carbide paper to a .05 μm alumina solution on polishing pads (see Table 7). Nikon NIS-Elements F2.30 imaging software in conjunction with a Nikon Optical Microscope Model Epiphot 200 was used to capture the microstructural images of the samples (see Figure 24).

Table 7.   Metallography parameters used to polish the AA5456 samples.

Metallography Parameters

Silicon—Carbide Disc [grit] / AlO$_3$ Solution on Polishing Pad [µm]	Polishing Time [min]	Load [N]	Rotation Speed [rpm]
1200 grit (disc)	5	35.6	80
2400 grit (disc)	10	26.7	80
5 µm (pad)	15	26.7	100
3 µm (pad)	15	26.7	100
1 µm (pad)	20	13.3	120
0.05 µm (pad)	20	13.3	120
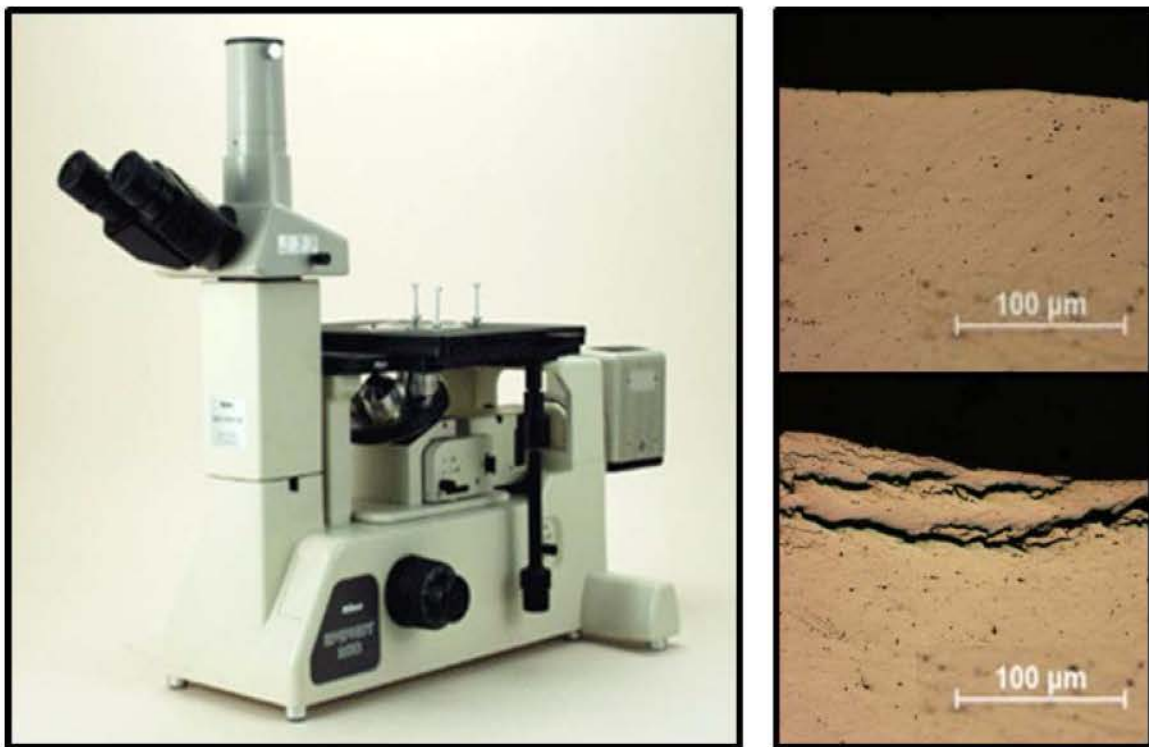
Figure 24.   Left: Nikon Optical Microscope Model Epiphot 200. Right: Example of two microstructural images taken at 10x magnification of AA5456 samples.

B.   FIELD-BASED EXPERIMENTS

Field-based experiments consisted of a systematic review of *in situ* metallography's effect on residual stress measurements of a non-sensitized AA5083 plate and residual stress measurements of welded AA5083 decks on-board a U.S. naval combatant. X-ray residual stress measurements were performed using a portable Proto-iXRD instrument.

1. Non-sensitized, Systematically Surface Prepared, Aluminum-Alloy 5083 Plate

To determine the effects of standard *in situ* surface preparations on residual stresses, a non-sensitized AA5083 plate was used. A Ryobi 5 inch orbital sander with a 120 grit sanding disc was used to perform the initial surface treatment on a 29.8 cm (11.75 in) wide by 43.2 cm (17 in) long portion of the 6 mm (.25 in) thick, 29.8 cm (11.75 in) wide and 60.3 cm (23.75 in) long AA5083 plate. Collaborators from NSWCCD systematically performed eight different surface preparations (120 grit, 240 grit, 500 grit, 600 grit, 1000 grit, 6 μm, 1 μm, .05 μm), each in an area of approximately 25.4 millimeters (1 inch) by 63.5 mm (2.5 inches) (see Figure 25 and Table 8) [32], [47].
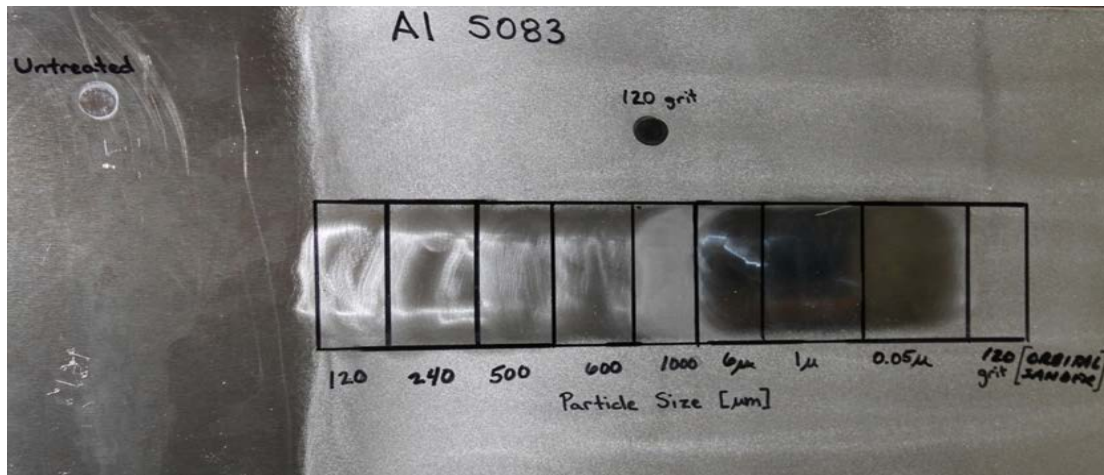
Figure 25.   Systematic surface preparations conducted by NSWCCD collaborators on a non-sensitized AA5083 plate.[2]

---

[2] Numbers 120 through 1000 are paper grit sizes and the remaining are particle sizes in a solution.

Table 8.   Conversion chart from grit designation to average particle size in micrometers.

Grit Conversion to Average Particle Size	
125 grit	115 μm
240 grit	53 μm
500 grit	20 μm
600 grit	16 μm
1000 grit	10.3 μm

Residual stress measurements were taken of each of the eight surface prepared areas along with an untreated (control) area of the non-sensitized AA5083 plate using the same x-ray diffraction conditions as in Table 5. To determine depth-resolved residual stresses, the plate received two electropolishing treatments, one in the control area, and another in the 120 grit surface treated area. The residual stresses of the two electro-polished areas were measured using MET as well.

2. Field-Based Residual Stress Measurements

Field-based residual stress measurements were performed on-board a U.S. Navy Combat Ship using the Proto iXRD Residual Stress Analyzer in an open-beam configuration. The XRD analyzer was operated in accordance with NPS Open-Beam SEOP and U.S. Navy radiation safety requirements. Measurements were recorded at three locations, Mission Bay Area 1, Mission Bay Area 2, and the Forecastle. Surface preparation was needed to remove any paint or surface imperfections that may have interfered with the residual stress measurements. The surfaces being tested at each location were prepared by collaborators from NSWCCD using *in situ* surface preparation procedures to a 0.05 μm polish (see Figure 26) [8], [17].
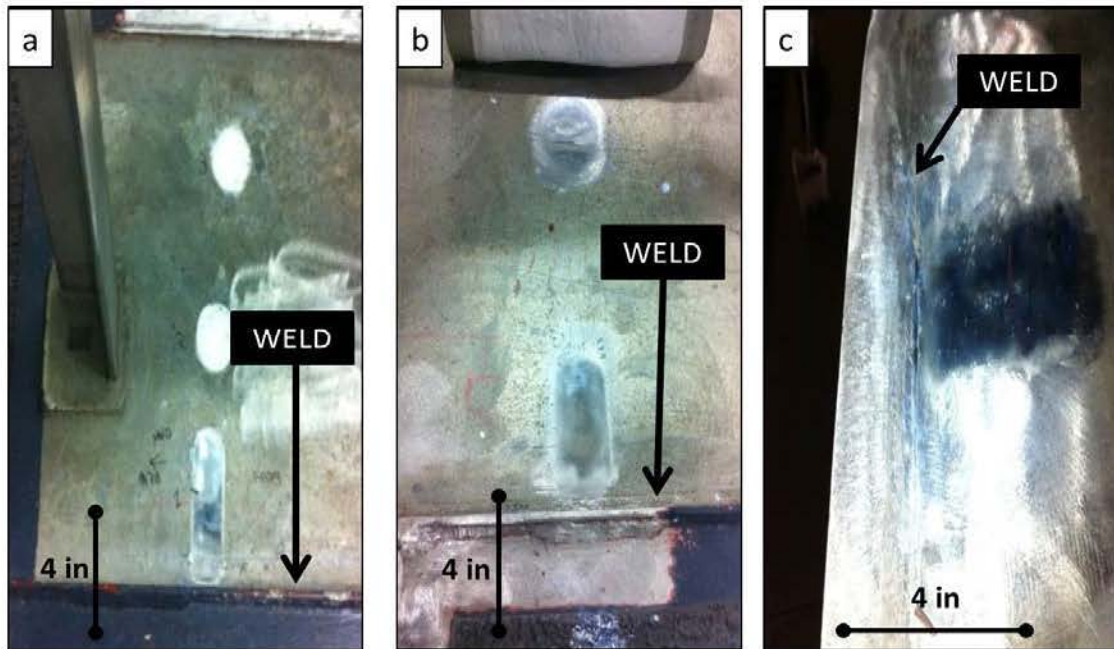
Figure 26.   Shipboard surface prepared areas. Image (a) is Mission Bay Area 1.
Image (b) is Mission Bay Area 2. Image (c) is of Area 3 on the outer
edge of the Forecastle.

Operating in an open-beam configuration required radiation safety boundaries to be erected in accordance with established operating procedures and U.S. Navy radiation safety requirements (see Figure 27). The following steps were completed prior to taking measurements:

- The thickness of the deck was confirmed using an ultrasonic transducer. To verify safety of personnel passing beneath the work area, a minimum thickness of 2 mm (0.079 in) was required. The standard deck thickness in these field measurements was 6.35 mm (0.25 in).
- All team members were required to wear personal dosimetry
- A radiation safety boundary was roped-off, and the area was posted for radiation at the required 1 meter radius in all directions to achieve an x-ray exposure rate of <2 mrem/hr.
- A radiation survey was conducted to confirm x-ray radiation levels of < 2mrem/hr at the boundary.
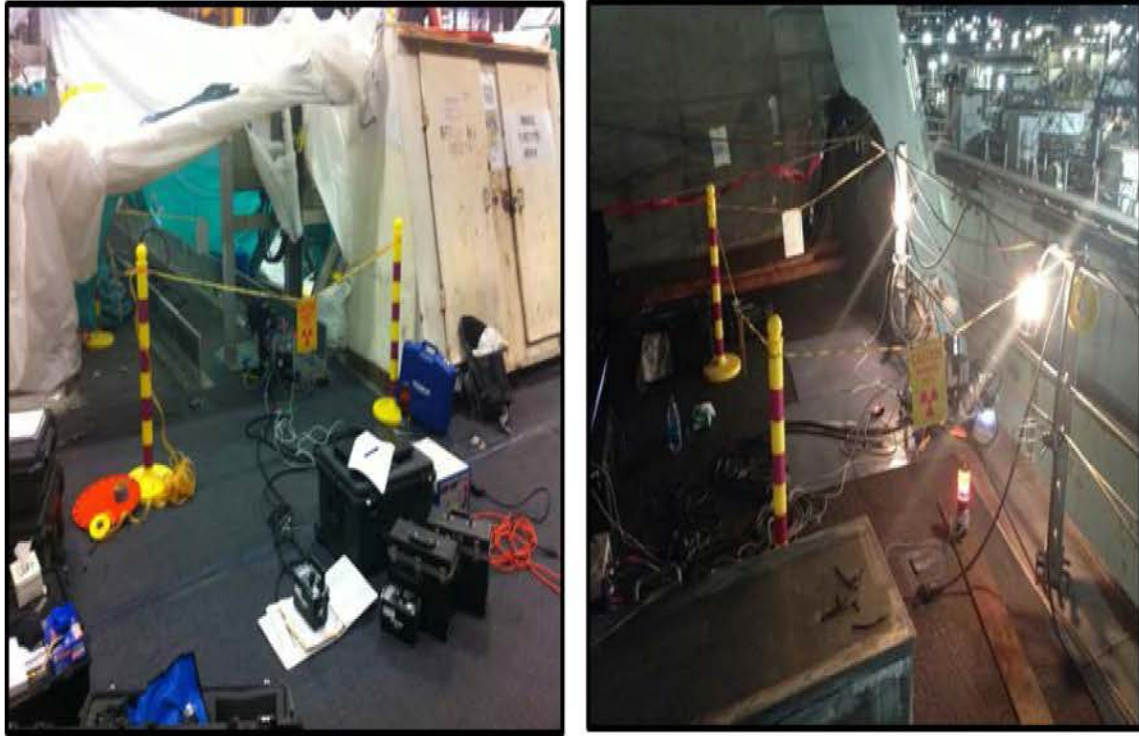
Figure 27.   Shipboard field setup of Proto iXRD and radiation safety equipment.
Image (a) is the setup in the Mission Bay. Image (b) is the setup on the
Forecastle.

Once all prerequisites for conducting the measurements were completed, a system alignment was conducted using the aluminum powder stress-free standard and the high-stress standard. This alignment verification was completed each time the machine was reassembled. The Proto analyzer was used to take residual stress measurements at each location transverse to the weld using the standard system parameters (see Table 9). Single residual stress measurements were collected at multiple locations in the mission bay for surface preparation effect comparisons. Residual stress line profiles were also taken at each location. The residual stress line profile measurements taken on the forecastle were taken both transverse and parallel to the weld line. To take the measurements parallel to the weld a phi angle of 90 degrees was used and the beta angle was adjusted from the standard 11 to 6 beta angles to accommodate the surface geometry and prevent damage to the Proto analyzer (see Figure 28).

Table 9.   Proto iXRD parameters for field-based residual stress measurements of AA5083 deck material on-board a U.S. Navy Ship.

	Mission Bay: Area 1 and 2	Forecastle: Area 3	
Tube Radiation Type	Cobalt K-alpha	Cobalt K-alpha	
Location of Detectors	Outside edge of knob at ~143 degree on arc	Outside edge of knob at ~143 degree on arc	
Data Collection Parameters	20kV, 4mA	20kV, 4mA	
Gain Parameters	10kV, 4mA	10kV, 4mA	
Aperture	2 mm diameter	2 mm diameter	
Beta Angle	11	11 Transverse	6 Parallel
Phi Angle	0	0 Transverse	90 Parallel
Exposures	5	5	
Exposure Time	5 seconds	5 seconds	
Exposure Gain	40	40	
Miller Index	{331} Reflection	{331} Reflection	
Bragg Angle	149 degrees	149 degrees	
Gain Shim	Beta Titanium	Beta Titanium	
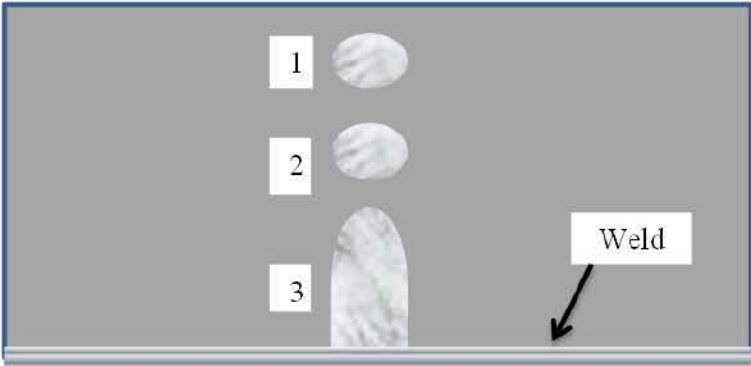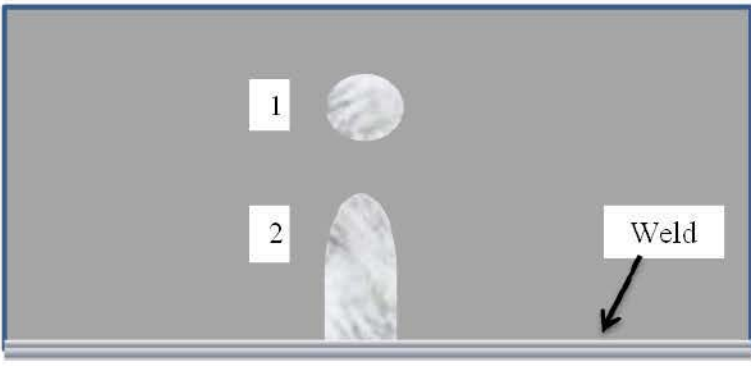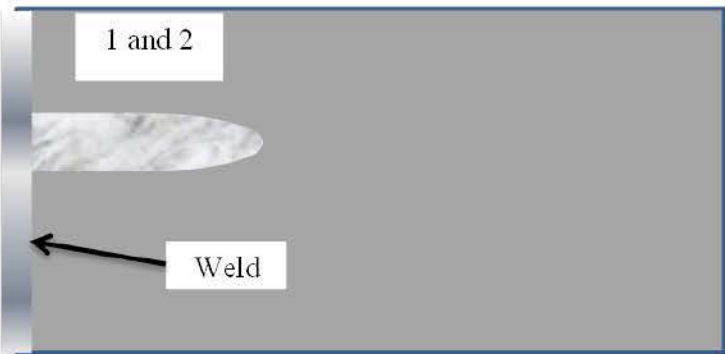
MISSION BAY: AREA 1		
	1	MET of a single point.
	2	MET of a single point.
	3	MET teach map of area. Line profile from weld out approximately 100 millimeters.

MISSION BAY: AREA 2		
	1	MET of a single point.
	2	MET teach map of area. Line profile from weld out to approximately 100 millimeters.

FORECASTLE: AREA 3		
	1	MET teach map of area. Line profile from weld out to approximately 35 mm. Six beta angles at phi set to 90°.
	2	MET teach map of area. Line profile from weld out to approximately 35 mm. Phi set to 0°.

Figure 28. Schematic of location and type of measurement taken, with respect to weld, at each area measured on-board a U.S. Navy Ship.[3]

---

[3] Multiple exposure technique (MET) is a Proto manufacturing specific term for residual stress measurement.

THIS PAGE INTENTIONALLY LEFT BLANK

III. RESULTS

A. X-RAY DIFFRACTION MEASUREMENTS

X-ray diffraction residual stress measurements were all performed using Proto Manufacturing iXRD instrument. Prior to taking each set of measurements, full alignment verification was performed using stress-free and high-stress aluminum standards in accordance with the Proto Manufacturing SEOP [44].

1. Systematically Ultrasonic Impact Treated, Gas Metal Arc Welded, Aluminum-Alloy 5456 Plates

The residual stress measurements of UIT treated zones across all parameters for both the sensitized and non-sensitized plates exhibited substantial compressive stresses (see Figure 29 through Figure 36). The residual stress measurements were taken from the toe of the weld out to approximately 100 mm from the weld. The magnitude of the compressive stresses over the measured area ranged from approximately -75 to -250 MPa. The UIT parameter of displacement amplitude played less of role than pin size did in the production of compressive residual stress in both the sensitized and non-sensitized plates. In general, with the exception of a few outliers (see Figure 35), all amplitudes and all pin sizes produced relatively high levels of compressive stresses across all UIT power inputs.

The sensitized plate at 60 percent power input exhibited the largest pin dependency on compressive stress values (see Figure 35). The use of a 1 mm pin at this power amplitude produced much larger compressive values than those generated with a 4 mm pin. The non-sensitized plate at 40 percent power input produced similar results, where the 4 mm pin generated lower compressive stress values than those produced when a 1 mm pin was used (see Figure 30). Unlike the consistent results for all pin sizes of the non-sensitized plate of the same power (see Figure 32), the sensitized plate at 80 percent power input, seen in Figure 36, shows compressive residual stresses began to decrease from roughly -150 to -70 MPa between 75 to 95 mm from the weld than increased back to approximately -150 MPa at the 100 mm from the weld. This was due to a non-

uniformly ultrasonic impact treated region. The non-sensitized plates averaged roughly -175 MPa for all pin sizes at 20, 60, and 80 percent power (see Figure 29, Figure 31 and Figure 32). The residual stresses averaged approximately -150 MPa regardless of pin size (see Figure 30). This may have been due to this section only receiving three UIT passes.

Figure 29.   Residual stresses of **non-sensitized** AA5456 taken at four zones, (Control, 1 mm, 3 mm, and 4 mm UIT pin diameter), with a 20 percent power input.
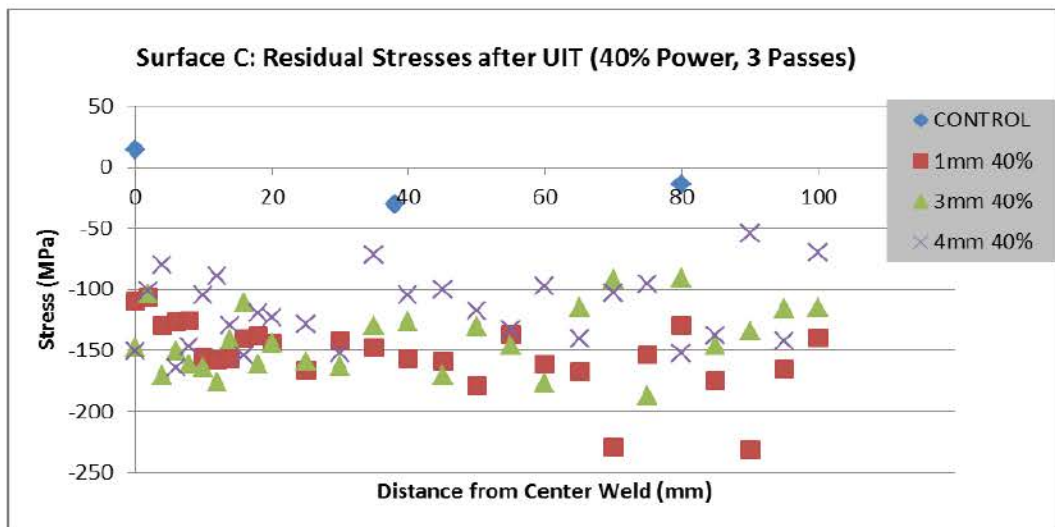
Figure 30.   Residual stresses of **non-sensitized** AA5456 taken at four zones, (Control, 1 mm, 3 mm, and 4 mm UIT pin diameter), with a 40 percent power input.

40
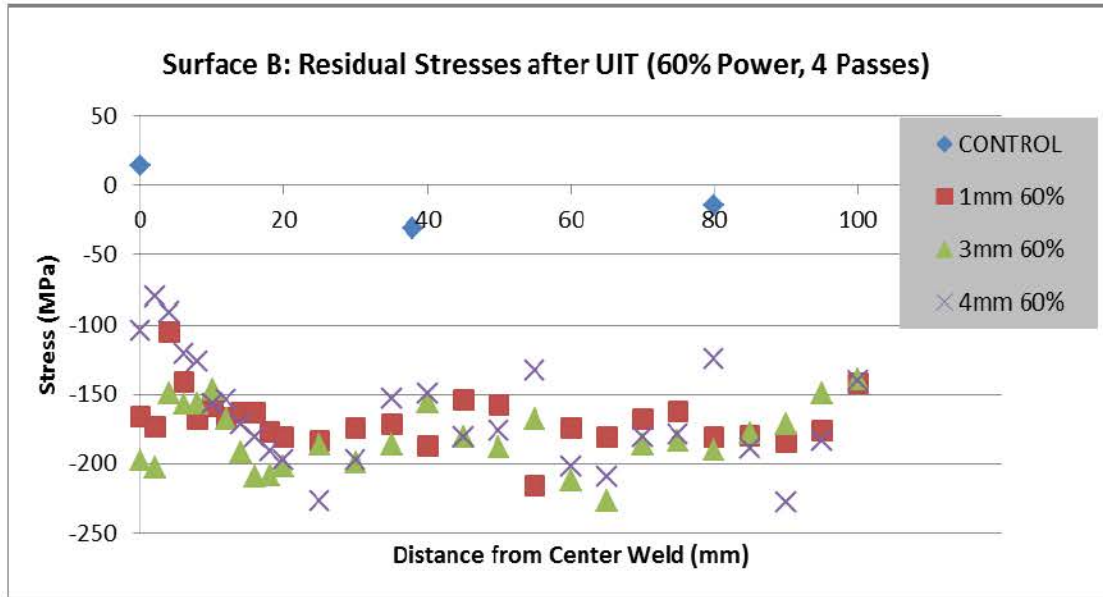
Figure 31. Residual stresses of **non-sensitized** AA5456 taken at four zones, (Control, 1 mm, 3 mm, and 4 mm UIT pin diameter), with a 60 percent power input.
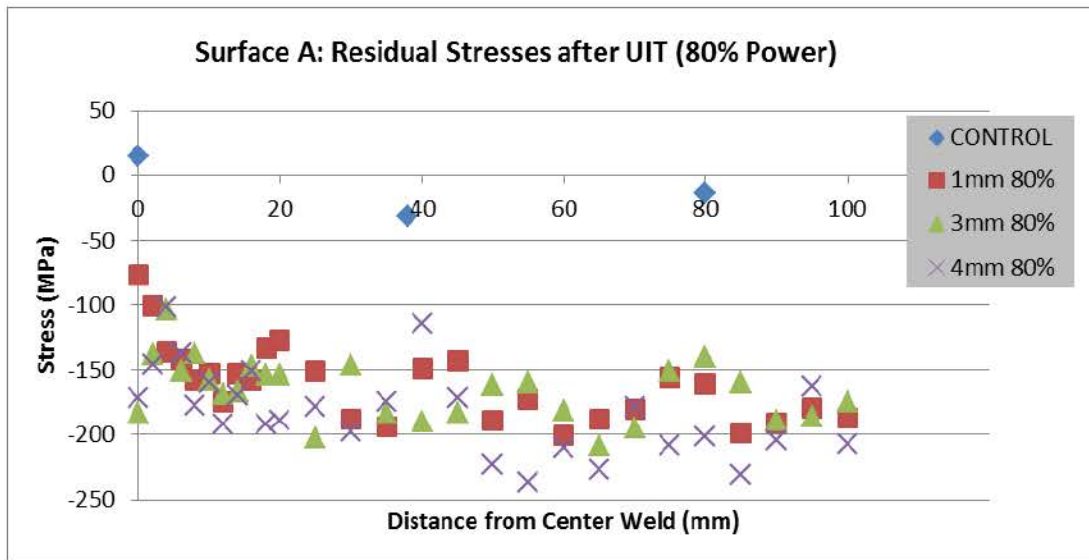
Figure 32. Residual stresses of **non-sensitized** AA5456 taken at four zones, (Control, 1 mm, 3 mm, and 4 mm UIT pin diameter), with an 80 percent power input.[4]

---

[4] UIT was measured in length of treatment time vice number of passes (4min@1mm pin, 3min@2mm pin, and 2min@1mm pin).

41
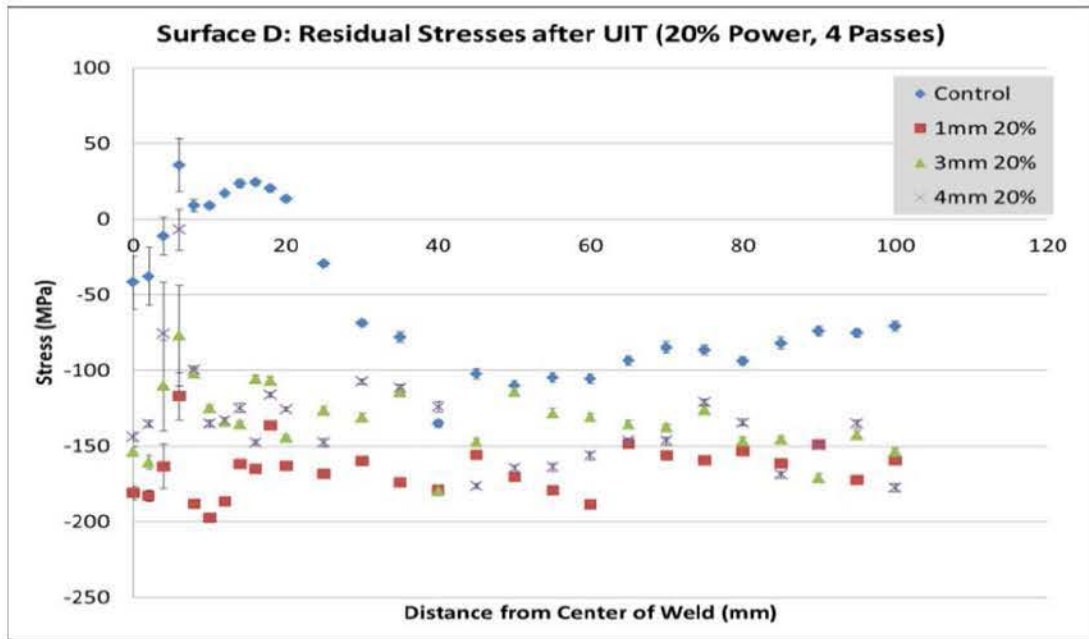
Figure 33.   Residual stresses of **sensitized** AA5456 taken at four zones,
(Control, 1 mm, 3 mm, and 4 mm UIT pin diameter), with a 20 percent
power input, from [13].
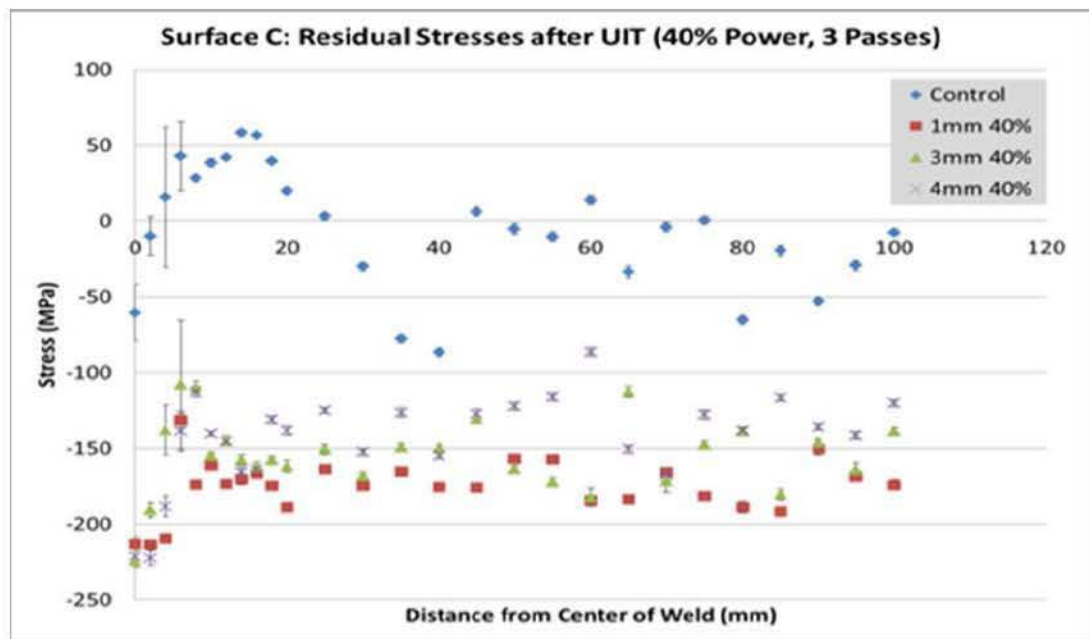
Figure 34.   Residual stresses of **sensitized** AA5456 taken at four zones,
(Control, 1 mm, 3 mm, and 4 mm UIT pin diameter), with a 40 percent
power input, from [13].
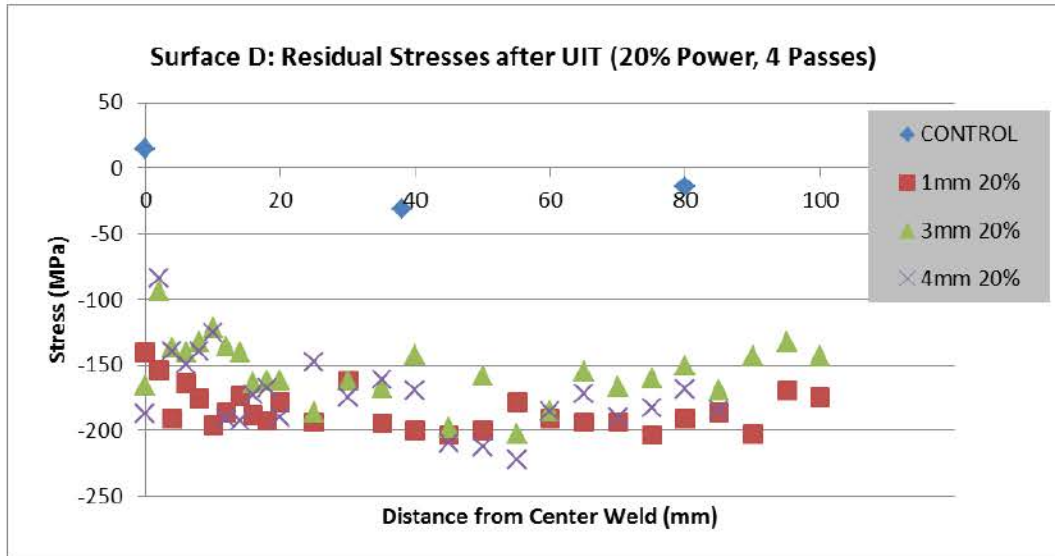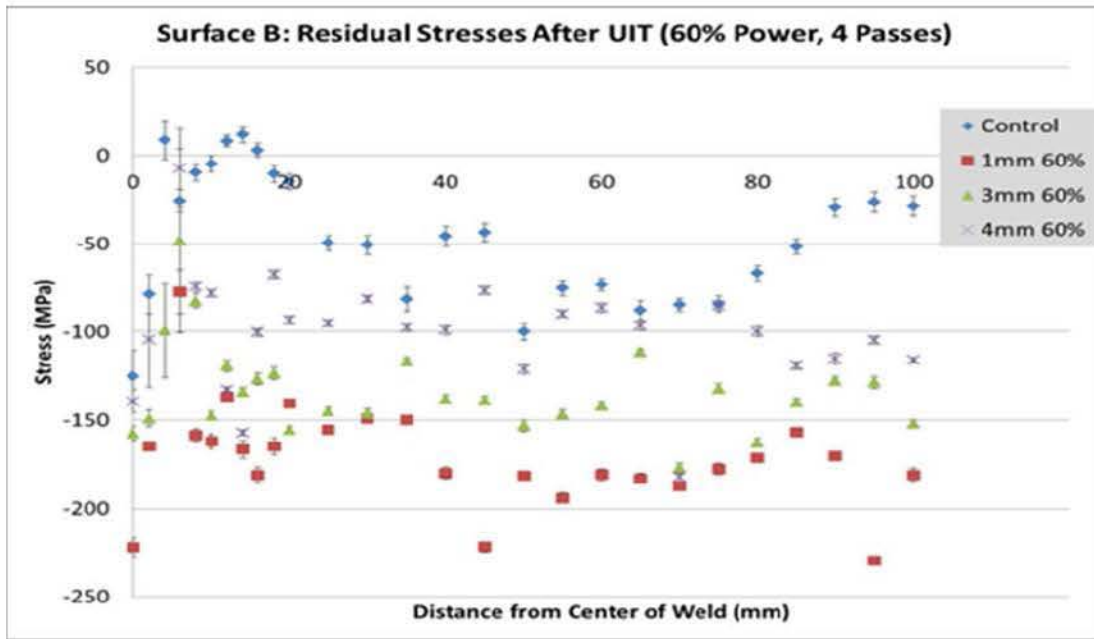
Figure 35.   Residual stresses of **sensitized** AA5456 taken at four zones, (Control, 1 mm, 3 mm, and 4 mm UIT pin diameter), with a 60 percent power input, from [13].
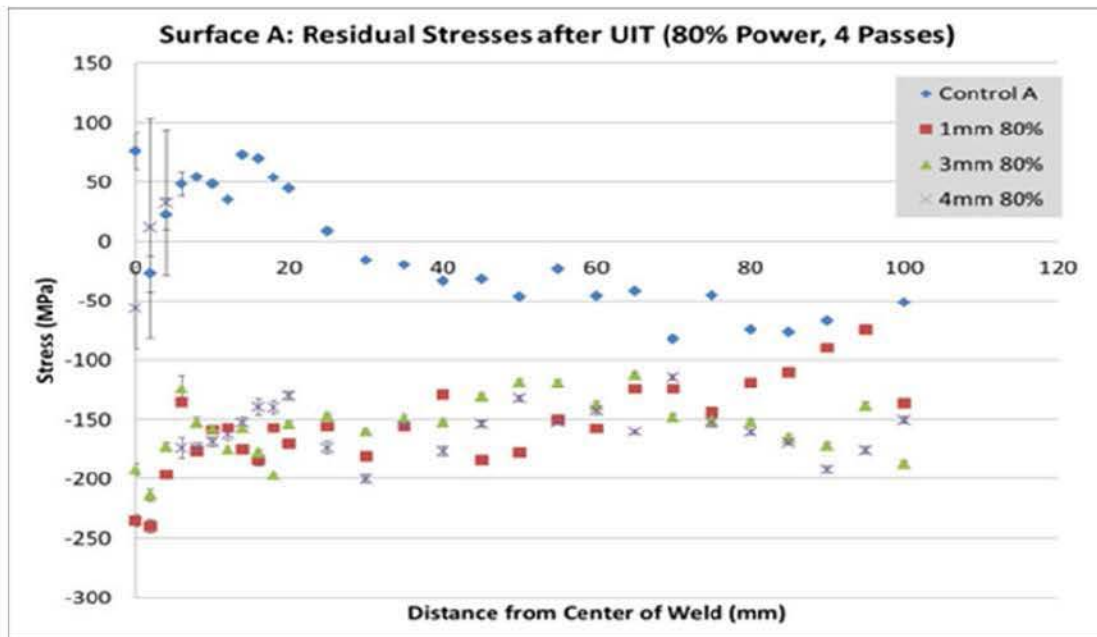
Figure 36.   Residual stresses of **sensitized** AA5456 taken at four zones, (Control, 1 mm, 3 mm, and 4 mm UIT pin diameter), with an 80 percent power input, from [13].

B.   OPTICAL MICROSCOPY

1.   Sensitized, Systematically Ultrasonic Impact Treated, Gas Metal Arc Welded, Aluminum-Alloy 5456 Samples

Optical microscopy showed sub-surface intergranular cracking for many of the UIT conditions applied to sensitized AA5456 samples. Each ultrasonic impact treated zone was analyzed for any evidence of microstructural deformations that may have occurred during the treatment. The images of the toe region were taken in the same location, approximately 4 to 6 mm from the toe of the weld. The heat effected zone images were taken from a region 6 to 15 mm from the toe of the weld. The most severe intergranular cracking was present at all pin sizes when using a 40 percent power input (see Figure 38). To note, the 40 percent power samples underwent only three UIT passes instead of 4 passes on the other areas. Micro-void formation occurred in the HAZ when a 60 percent power input with a 3 mm pin was used (see Figure 39). Inconsistent results were detected in the 80 percent power input samples. Severe intergranular cracking was present in the toe region but not the HAZ at 1 mm pin diameter at 80 percent power. The opposite was observed when using a 4 mm pin, where severe intergranular cracking was observed in the HAZ and none in the toe region (see Table 10).

The UIT power input and pin size to avoid the formation of sub-surface intergranular cracking were observed in Figure 37 through Figure 40. The optimal UIT parameters, where no cracks were generated, were in both the 20 percent power input sample with a 3 mm or 4 mm pin and in the 60 percent power input sample when a 4 mm pin was used. Table 10 provides an overview of cracking generated during all tested UIT parameters of the sensitized AA5456 samples. The right two columns of the table provide a simple go/no-go indication of if cracking was or was not present in the HAZ or toe region of the samples. The green indicates no cracks were found anywhere in the observed region and red signifying cracks were present.

Figure 37. Optical microscopy images of the HAZ and toe regions of **sensitized** AA5456 that have experienced UIT at 20 percent power input with varied pin sizes. From Top: 1 mm pin, 3mm pin, 4mm pin.

Figure 38.   Optical microscopy images of the HAZ and toe regions of **sensitized** AA5456 that have experienced UIT at 40 percent power input with varied pin sizes. From Top: 1 mm pin, 3mm pin, 4mm pin.

Power: 60%	Pin Diameter: 1mm
HAZ	**Toe**
Intermittent intergranular cracking only present in the HAZ.	

Power: 60%	Pin Diameter: 3mm
HAZ	**Toe**
Intermittent minor intergranular cracking present throughout. At ~15mm from Toe, micro-void formation just below surface.	

Power: 60%	Pin Diameter: 4mm
HAZ	**Toe**
No cracking present.	

Figure 39.   Optical microscopy images of the HAZ and toe regions of **sensitized** AA5456 that have experienced UIT at 60 percent power input with varied pin sizes. From Top: 1 mm pin, 3mm pin, 4mm pin.

Power: 80%	Pin Diameter: 1mm
HAZ	Toe

Severe intergranular cracking present at Toe but not in the HAZ.

Power: 80%	Pin Diameter: 3mm
HAZ	Toe

Intermittent intergranular cracking throughout HAZ but not at Toe.

Power: 80%	Pin Diameter: 4mm
HAZ	Toe

Severe intergranular cracking present throughout HAZ but not at Toe.

Figure 40. Optical microscopy images of the HAZ and toe regions of **sensitized** AA5456 that have experienced UIT at 80 percent power input with varied pin sizes. From Top: 1 mm pin, 3mm pin, 4mm pin.

48

Table 10.   Overview of cracking generated during all tested UIT parameters on sensitized AA5456 samples. Green indicates no cracks were observed. Red indicates cracks were present.

Sensitized AA5456 UIT Overview					
UIT Parameters		Cracking Observed			
Power Input [%]	Pin Size [mm]	HAZ [H]	Toe [T]	[H]	[T]
20	1	Yes	None	🟥	🟩
20	3	None	None	🟩	🟩
20	4	None	None	🟩	🟩
40	1	Yes – Severe throughout	Yes – Severe	🟥	🟥
40	3	Yes – Severe throughout	Yes – Severe	🟥	🟥
40	4	Yes	Yes	🟥	🟥
60	1	Yes	None	🟥	🟩
60	3	Yes – intermittent (micro-voids)	Yes	🟥	🟥
60	4	None	None	🟩	🟩
80	1	None	Severe	🟩	🟥
80	3	Yes	Yes	🟥	🟥
80	4	Yes – Severe intermittent	None	🟥	🟩

49

2. Non-Sensitized, Systematically Ultrasonic Impact Treated, Gas Metal Arc Welded, Aluminum-Alloy 5456 Samples

Optical microscopy did not show cracking or microstructural abnormalities after UIT for any of the non-sensitized AA5456 samples. Figure 41 displays optical images of two extremes in UIT parameters; the top two images are of samples that experienced UIT at a 20 percent power input with a 4mm pin (lowest contact stress) and the bottom two images are of samples that experienced UIT at an 80 percent power input with a 1 mm pin (highest contact stress). No cracking was observed in either the weld-toe or HAZ regions.
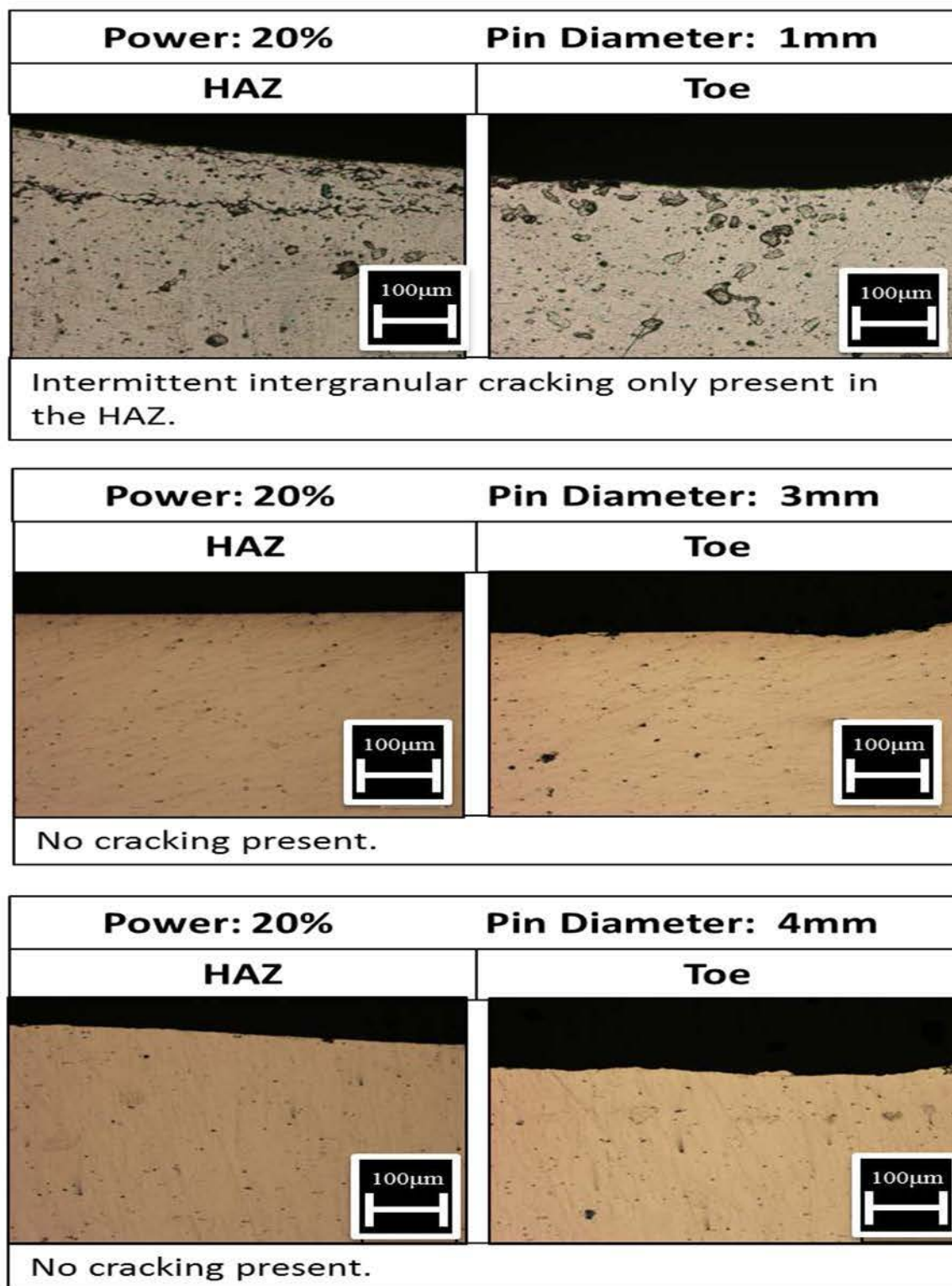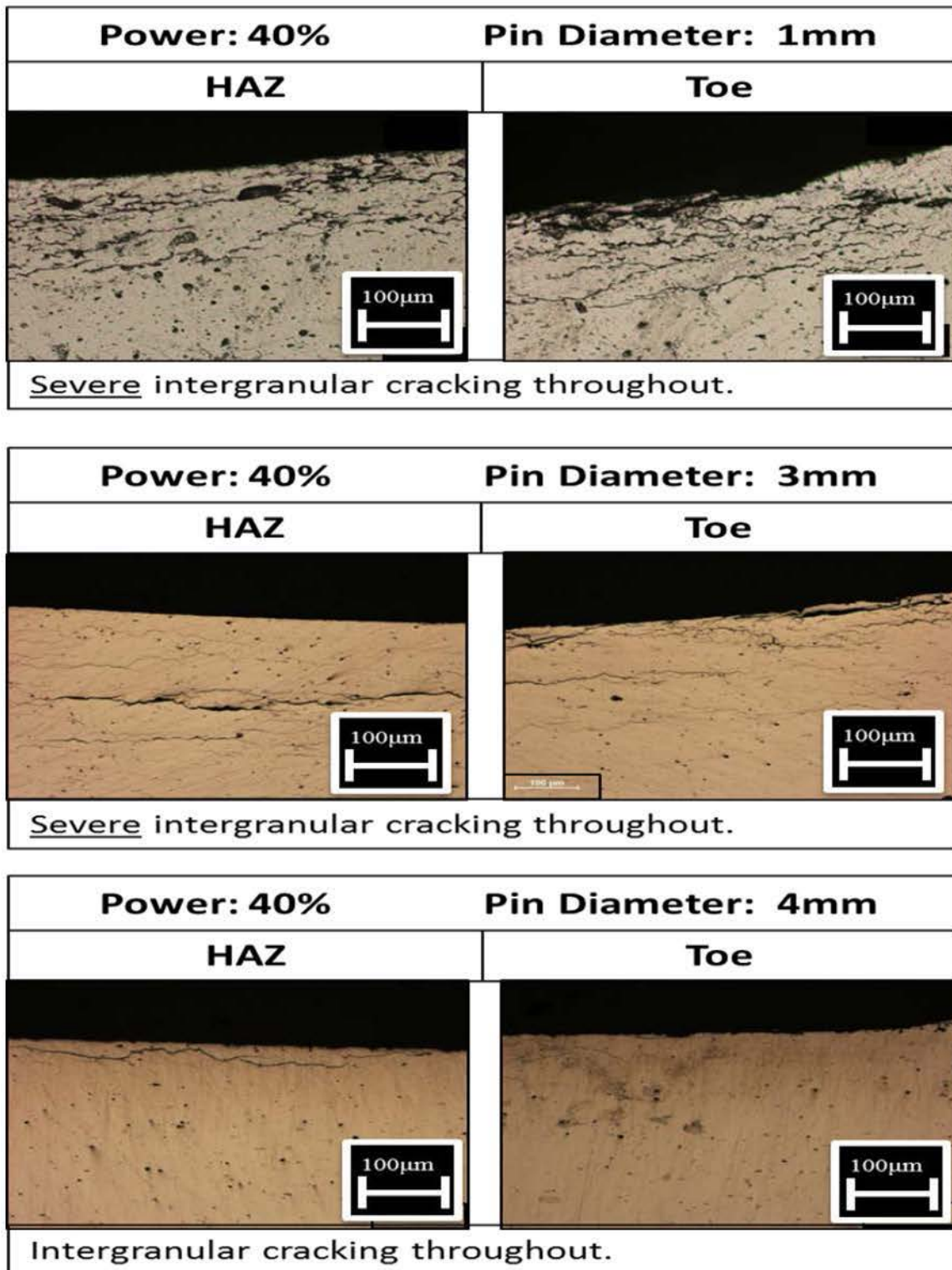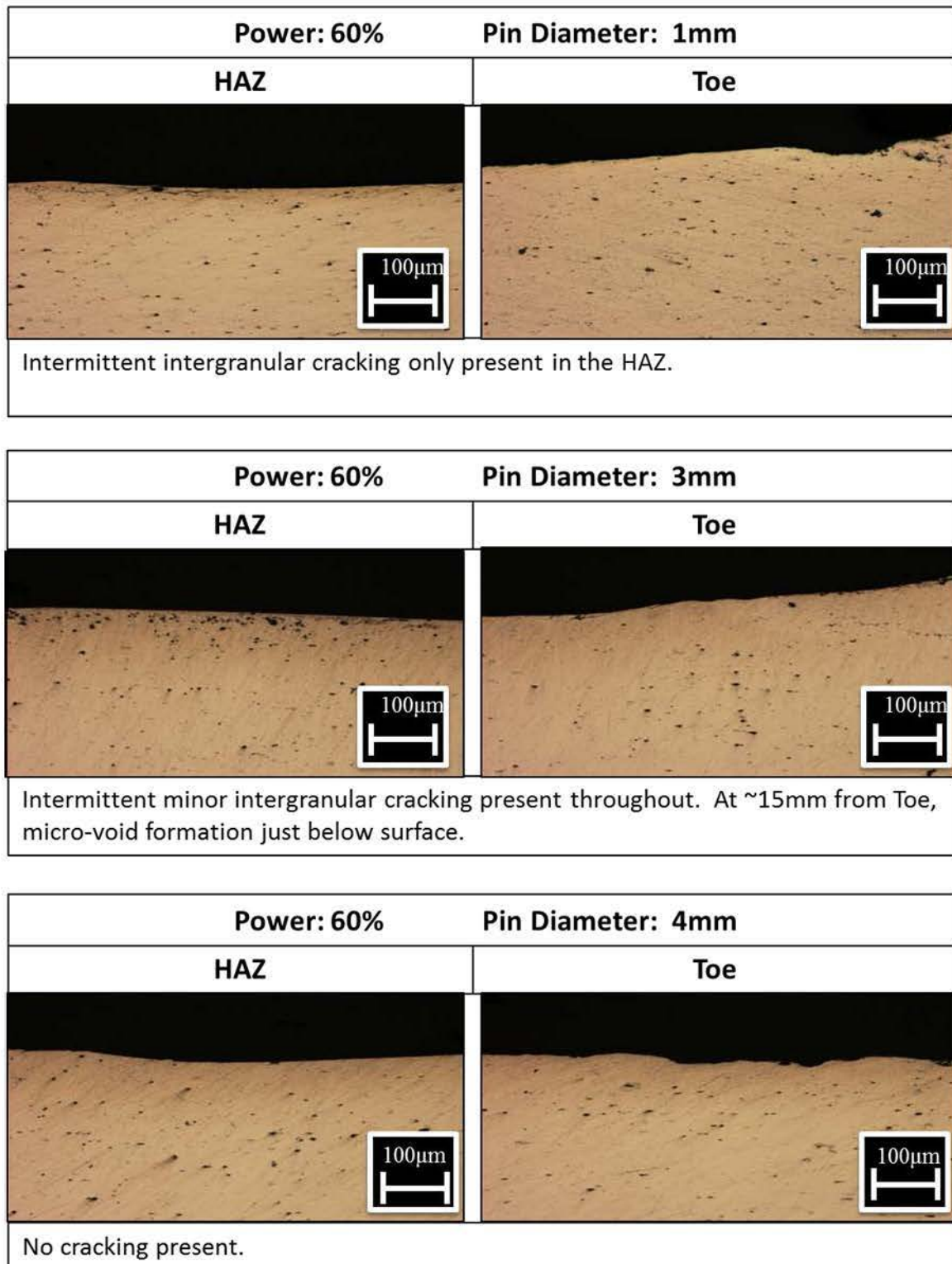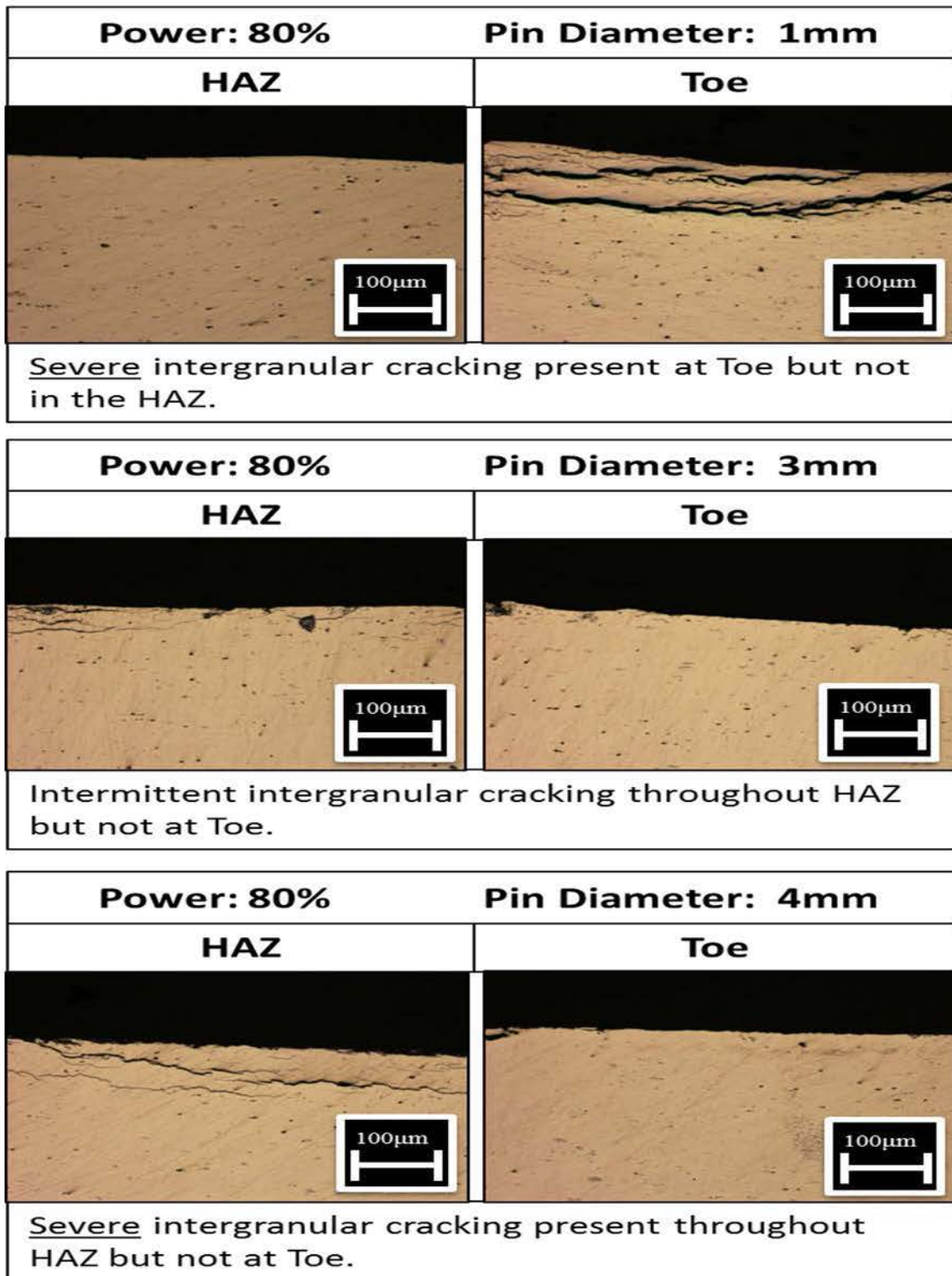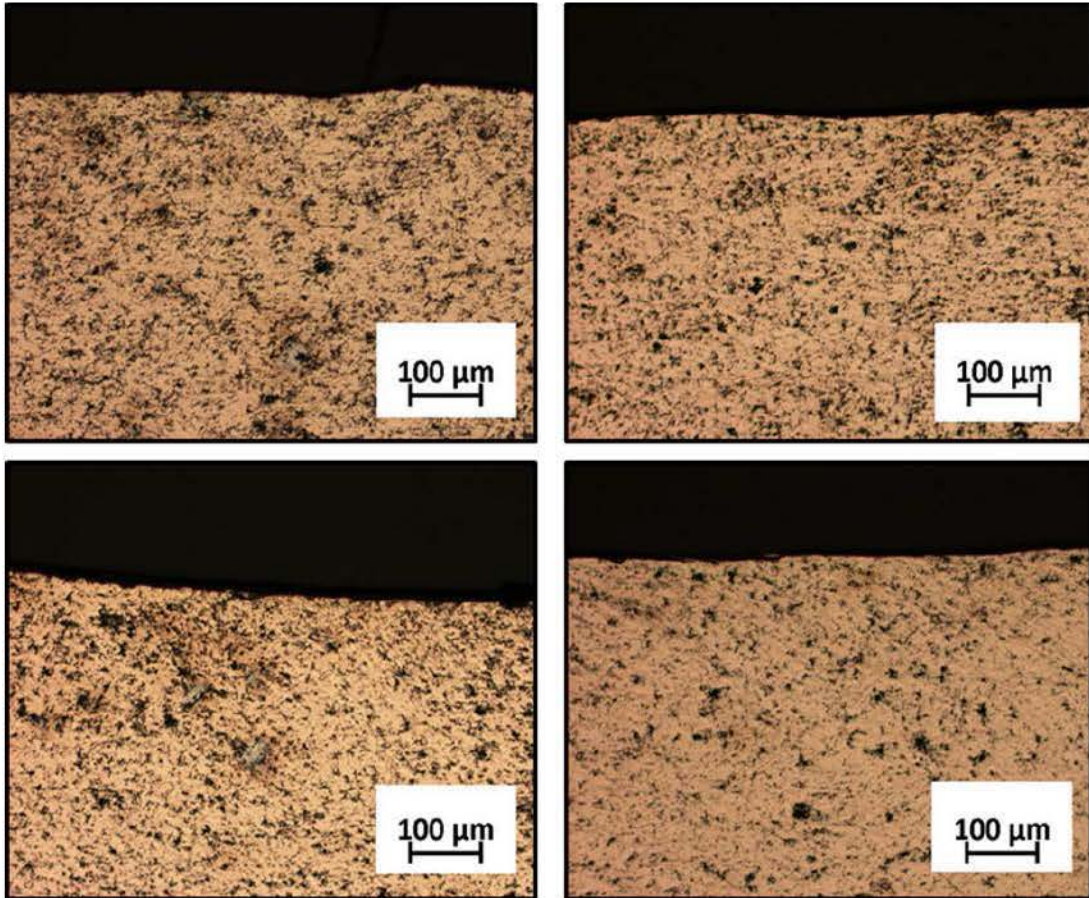

Figure 41.   Optical microscopy images of the HAZ and toe region of **non-sensitized** AA5456 that have experienced UIT at 20 and 80 percent power input and varied pin sizes. Clockwise from top left: 20 percent with 4 mm pin – weld toe, 20 percent with 4 mm pin – HAZ, 80 percent with 1 mm pin – HAZ, 80 percent with 1 mm pin – weld toe.

C. FIELD-BASED MEASUREMENTS

Field-based experiments consisted of a systematic review of *in situ* metallography's effect on residual stress measurements of a non-sensitized AA5083 plate and residual stress measurements of welded AA5083 decks on-board a U.S. naval combatant. X-ray residual stress measurements were performed using a portable Proto-iXRD instrument.

1. Non-sensitized, Systematically *In Situ* Surface Prepared, Aluminum-Alloy 5083 Plate

Residual stress measurements of the plate (see Figure 42) clearly indicate *in situ* surface preparations affect field measurements. Compressive stresses ranging between roughly -22 to -53 MPa were generated regardless of the particle size of the surface preparation, polishing pad, or solution used (see Figure 43). The 10.3 μm grit paper generated higher compressive stresses relative to coarser grit paper used to grind. This difference may be due to cross contamination due to improper cleaning of the surface between grinding phases. In the region of the plate where no *in situ* treatments were applied, the residual stresses measured were around 12 MPa (tensile). To note, when the mean value of measured stress is below 14 MPa, it is considered approximately zero [1]. The largest compressive value of -53 MPa was generated when a 120 grit (115 μm particle) grinding paper was used. Interestingly, polishing did not fully remove the compressive residual stresses on the surface.
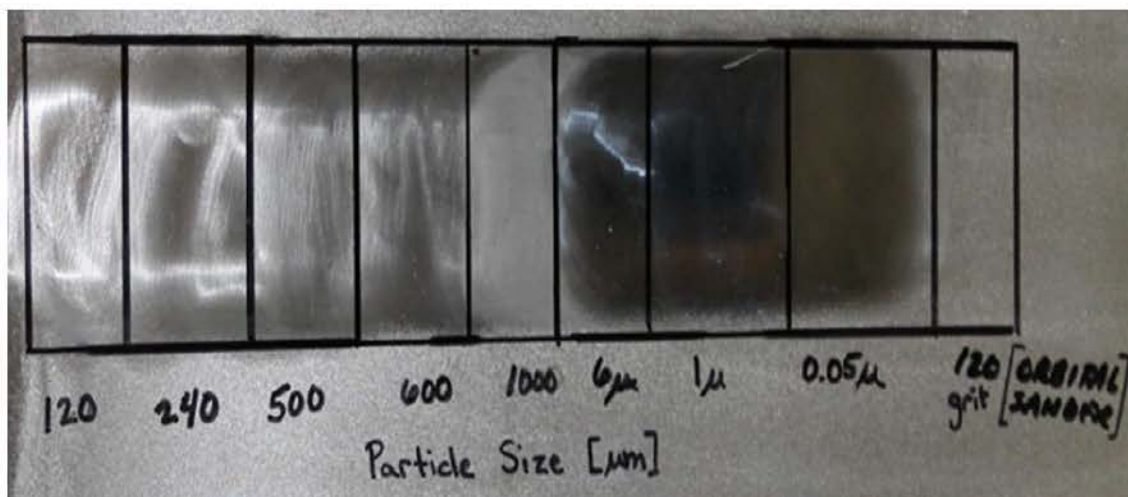
Figure 42.   Systematic surface preparations conducted by NSWCCD collaborators on a non-sensitized AA5083 plate.[5]
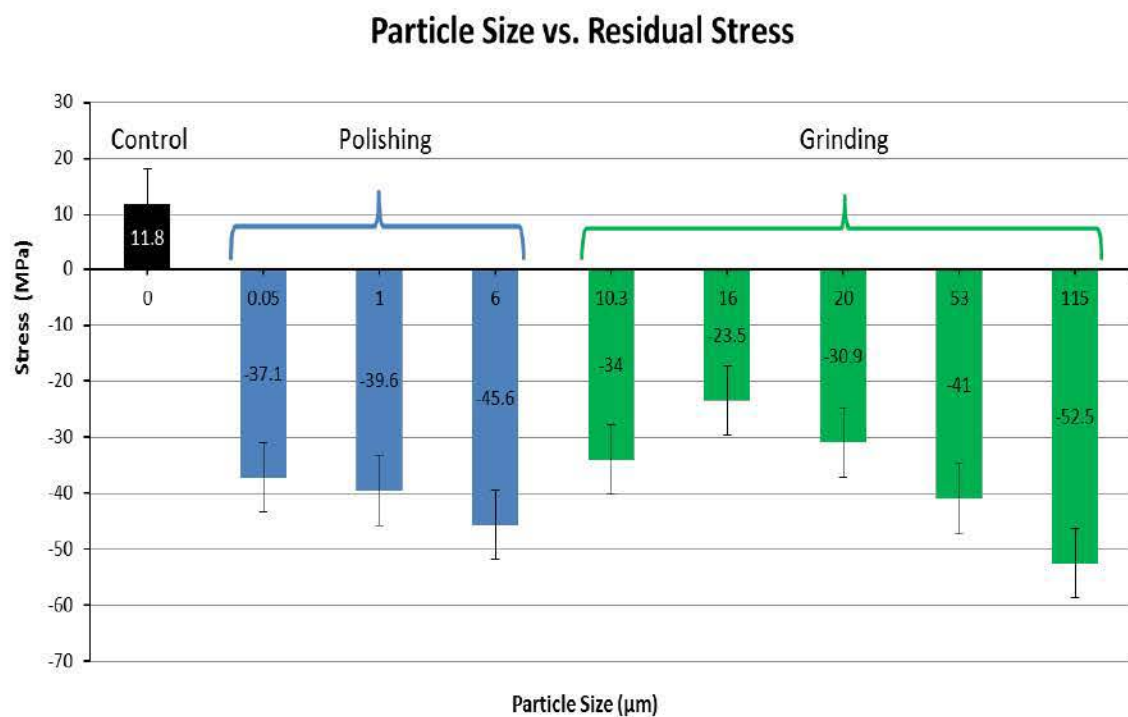
Figure 43.   Residual stress measurements of **non-sensitized** AA5083 after *in situ* surface preparations were performed.

---

[5] The numbers 120 through 1000 are paper grit size and the remaining are the size of particles in a solution.

Residual stress measurements were taken at two areas of a non-sensitized AA5083 plate before and after electropolishing. The first area was untreated, representing the control area of the plate, and the surface of the second area was ground using an orbital sander with a 120 grit disc (see Figure 44). Prior to electropolishing, the untreated surface was measured to have 11.8 MPa (tensile) of residual stresses present. The grinding of the plate generated compressive stresses of -52.5 MPa. After electropolishing to a depth of roughly between 500 and 1000 μm, residual stress measurements indicated that both the untreated and treated areas produced relatively the same stress value, 19.3 +/- 4.7 MPa and 18.4 +/- 4.1 MPa respectively (see Table 11). This result suggests that the 120 grit grinding deformed the surface and introduced residual stresses.
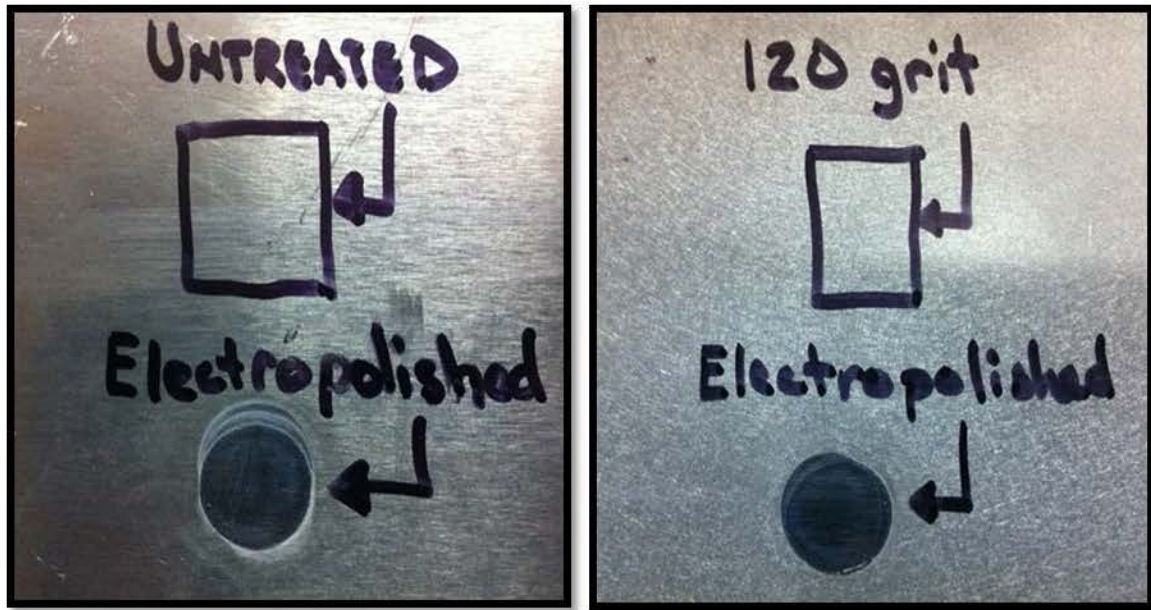
Figure 44. Pictured are two sections of the same non-sensitized AA5083 plate, both with an electropolished area.

Table 11. Before and after results of residual stress measurements of two electropolished areas of a non-sensitized AA5083 that underwent different surface treatments.

	Before Electropolishing	After Electropolishing
	Untreated (Control) Surface	
σ	11.8 +/- 2.6 [MPa]	19.3 +/- 4.7 [MPa]
τ	1.0 +/- 1.2 [MPa]	-4.2 +/- 2.2 [MPa]
	120 Grit Treated	
σ	-52.5 +/- 8.3 [MPa]	18.4 +/- 4.1 [MPa]
τ	-20.2 +/- 4.0 [MPa]	-2.5 +/- 1.9 [MPa]

2. Field-Based Residual Stress Measurements

(1) Mission Bay, Area 1:

The residual stresses were measured in an *in situ* surface prepared area, polished to 0.05 μm, on a welded AA5083 deck plate. Stress measurements were collected in a line profile from the toe of the weld out to 120 mm from the weld. Close to the weld toe (from the weld toe out to approximately 10 mm), the measured longitudinal (parallel to the weld) stresses were slightly compressive, between roughly -20 and -30 MPa, (see Figure 45). Proceeding out from the weld, the stresses became slightly positive, measuring just over 5 MPa around 12 mm from the weld, before becoming significantly more compressive at approximately 19 mm from the toe region of the weld. The larger compressive stresses continued for the remainder of measured areas out to 120 mm from the weld.

Residual Stress Measurements in AA5083 Deck Plate: MISSION BAY AREA 1
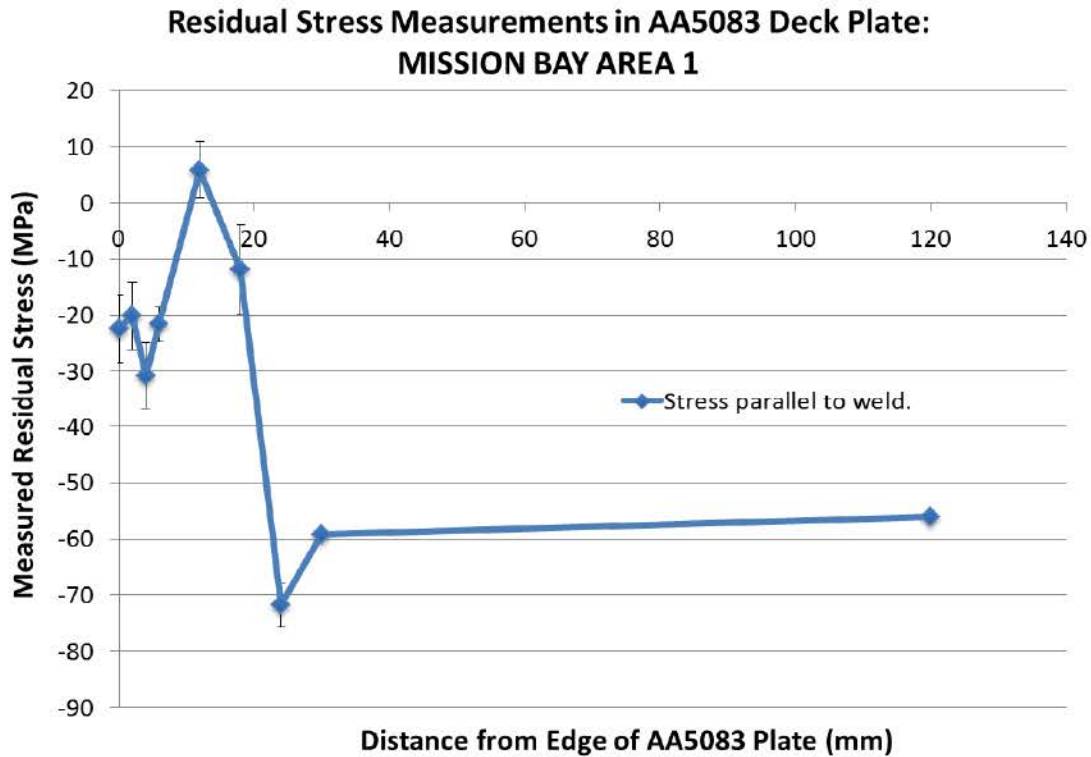
Figure 45.   Residual stresses in the Mission Bay (Area 1) of AA5083 deck plate on-board a U.S. Navy ship.

(2)   Mission Bay, Area 2:

The geometry and location of the measured welds in this area allowed for the opportunity to perform x-ray diffraction both parallel and transverse to the weld. The measured surface in this region also underwent *in situ* surface preparation to a 0.05μm polish. The longitudinal (parallel to the weld) stresses were nearly zero next to weld becoming more compressive the further way from the weld the measurements were taken. The compressive stresses leveled off at approximately 40 mm from the weld, maintaining a value roughly in the range of -40 to -50 MPa (see Figure 46). For the first 40 mm from the weld, the transverse (perpendicular to the weld) stresses were not measured due to surface obstructions near the weld. Transverse stresses were much more compressive than the longitudinal stresses.
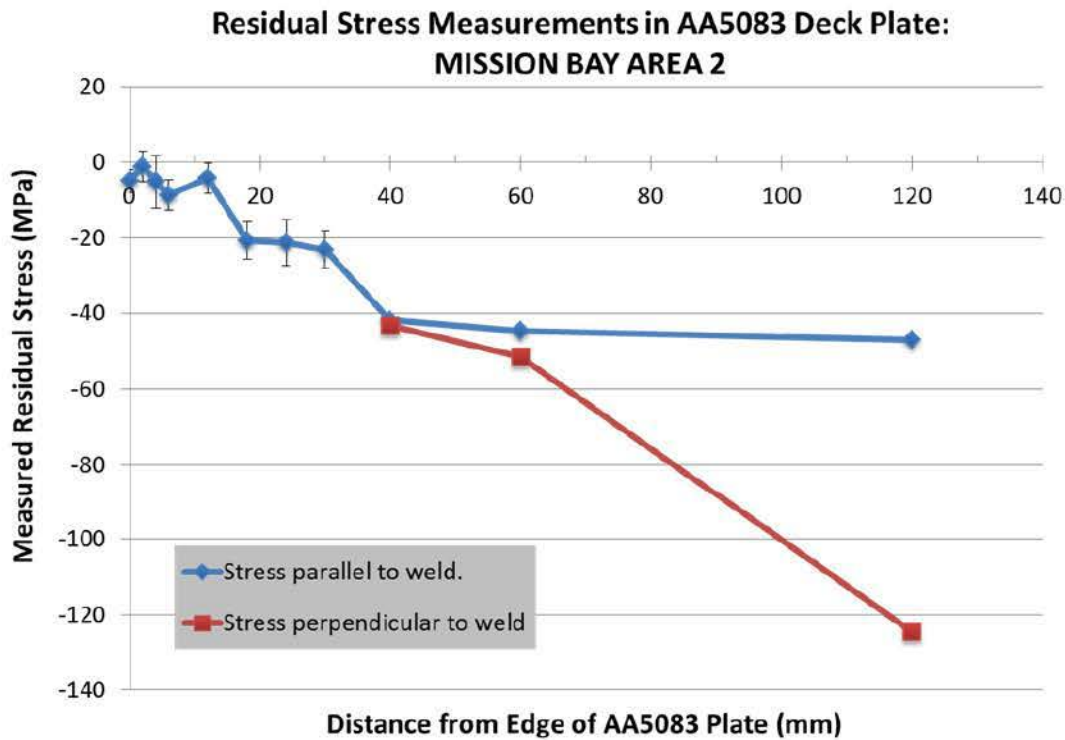
Figure 46.   Residual stresses measured in the Mission Bay (Area 2) of AA5083 deck plate on-board a U.S. Navy ship.

(3)   Forecastle, Area 3:

Residual stresses were measured on the deck plate installed on the forecastle both longitudinally and transverse to the weld. The longitudinal (parallel) stresses began slightly positive at the weld toe, just over 16 MPa, but then quickly became compressive and remained relatively constant, ranging from roughly -40 to -82 MPa with one much more compressive outlier at 18 mm from the weld, which reached approximately -110 MPa (see Figure 47). The transverse (perpendicular) stresses were all compressive, beginning with -100 MPa near the weld then becoming less compressive until reaching approximately 28 mm from the weld when it became much more compressive. Due to the geometry and location of the deck plate on the forecastle, only 6 beta angles were taken and the Proto iXRD could only maneuver out to 30 mm from the weld. An unexpected dip in residual stress occurs in both the transverse and longitudinal measurements in the polished region at 18 mm from the weld.

56
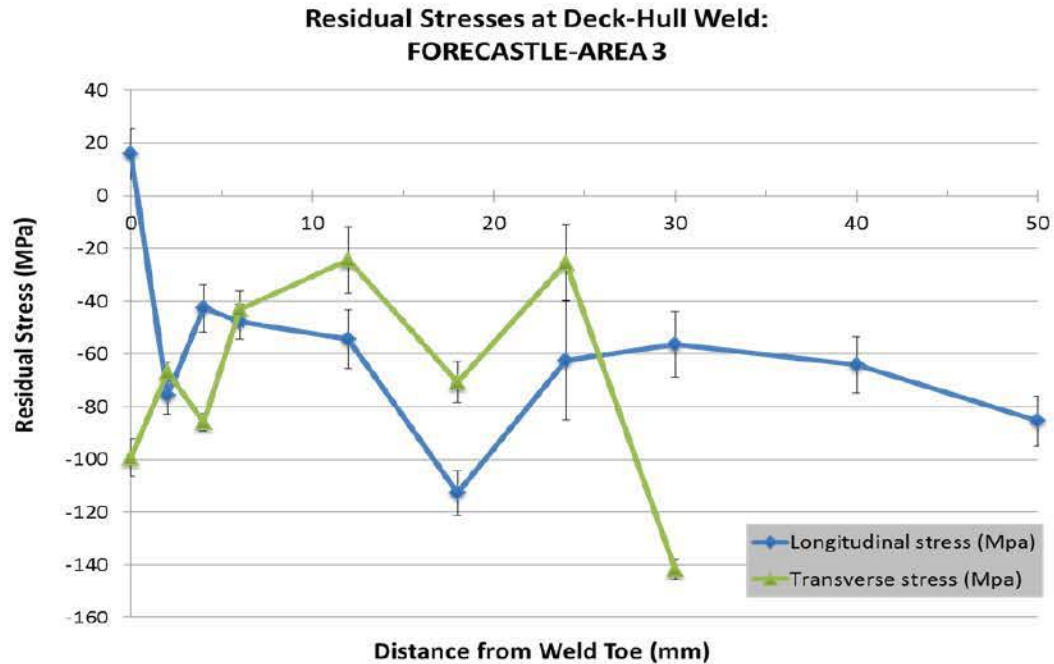
Figure 47.   Residual stresses on the forecastle (Area 3) of AA5083 deck plate
on-board a U.S. Navy ship.

For further comparison of the transverse residual stress measurements near the weld on the forecastle, transverse residual stress measurements at two additional unpolished locations were taken. The unpolished areas were untouched and measured as found [48]. The two unpolished areas measured, represented by the green and red curves in Figure 48, show that compressive stresses were observed whether or not the area was polished. Both unpolished areas remained fairly constant throughout, with the exception of one measurement at 12 mm from the weld of the first unpolished area, which reached -141.8 MPa. The second unpolished area (**red curve**) was only measured out to distance of 12 mm from the weld due to XRD space limitation around that area of the forecastle.
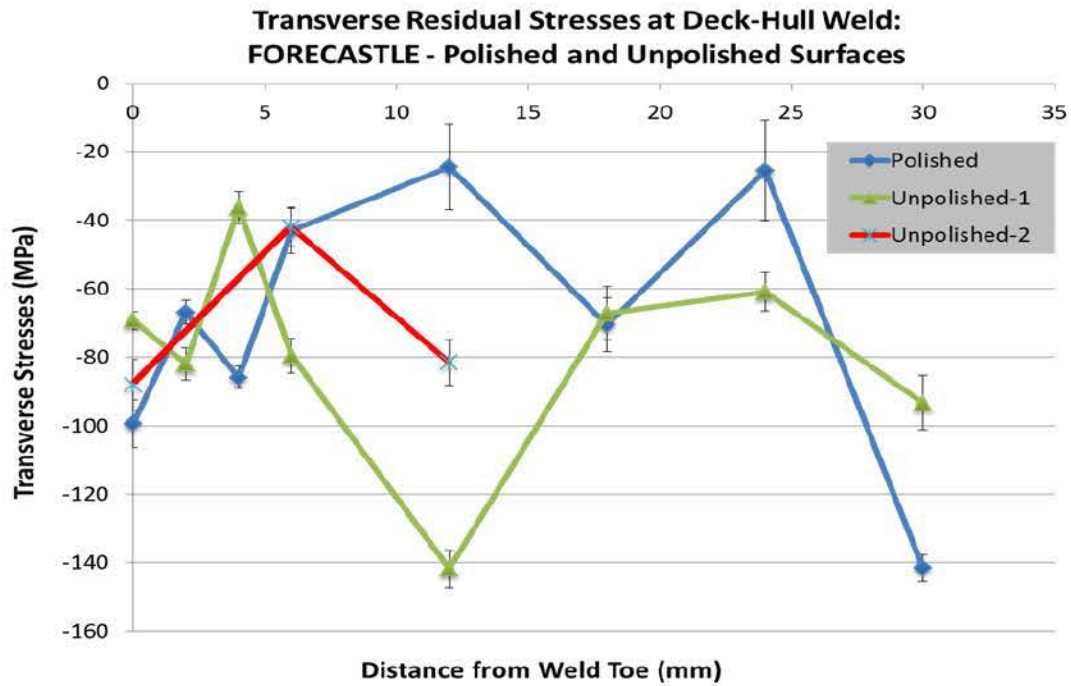
Figure 48. Residual stresses on the forecastle (Area 3) at three locations of AA5083 deck plate-hull weld on-board a U.S. Navy Ship.

IV.   DISCUSSION

In this thesis, we measured and analyzed compressive stresses generated after UIT in sensitized and non-sensitized AA5456 and found that, if sensitized, lower compressive stresses were generated under most UIT parameters. Peening techniques, such as UIT used in this thesis, are commonly used to mitigate tensile stresses generated by GMAW in AAs. Across all UIT parameters tested, compressive stresses were generated, ranging from -50 to -250 MPa in the aluminum-alloy under both sensitization conditions. Compressive stress values observed in the non-sensitized AA5456 plates were less variable then those produced in the sensitized plates (see Figure 29 through Figure 36). This is most evident when analyzing the non-sensitized plates starting from approximately 10 mm from the toe of the weld out to 100 mm, where the collected x-ray diffraction data remained in a comparatively close-fitting set of compressive values regardless of pin size or percent power input (see Figure 29 through Figure 32). The average of the compressive stresses induced on all surfaces after UIT of the sensitized plates was approximately -140 MPa [13], whereas ultrasonic treatment of the non-sensitized plates generated an average of -161 MPa. The one exception for the sensitized plates were the residual stresses generated at the 1 mm pin/80% power condition—these stresses were comparable to those observed in the non-sensitized plates. Research conducted on the effect of sensitization on AAs by Oguocha et al. [18] found that sensitization of a material lowered its overall yield strength [18]. As a material's yield strength decreases, the level of residual stress that it can support also decreases. Although the average residual stress values are relatively close, the 13 percent decrease in magnitude of average stress shows the effect sensitization plays in the generation of compressive stress.

A comparison of the average residual stresses generated during UIT suggests that pin size and displacement amplitude do not strongly influence the magnitude of compressive stresses (see Figure 49). With the exception of a few outliers, a 1 mm pin produced the largest compressive stresses averaging -166 MPa across all tested areas and UIT parameters with the 3 mm and 4 mm pin following closely behind with an average of

-161 MPa and -156 MPa respectively. Residual stress differences of less than 10 MPa are not measurably different, suggesting pin size does not significantly affect the residual level in the plate material. In contrast, the average residual stresses in the heat affected zone of the weld (edge of weld out to approximately 8 mm), where the majority of heat effects from welding occur, we find compressive stress levels of the non-sensitized plates were consistently higher across all UIT parameters (see Figure 50). The exact reason for the decrease in stress for sensitization is unclear but may be related to the reduction in yield strength that accompanies sensitization.
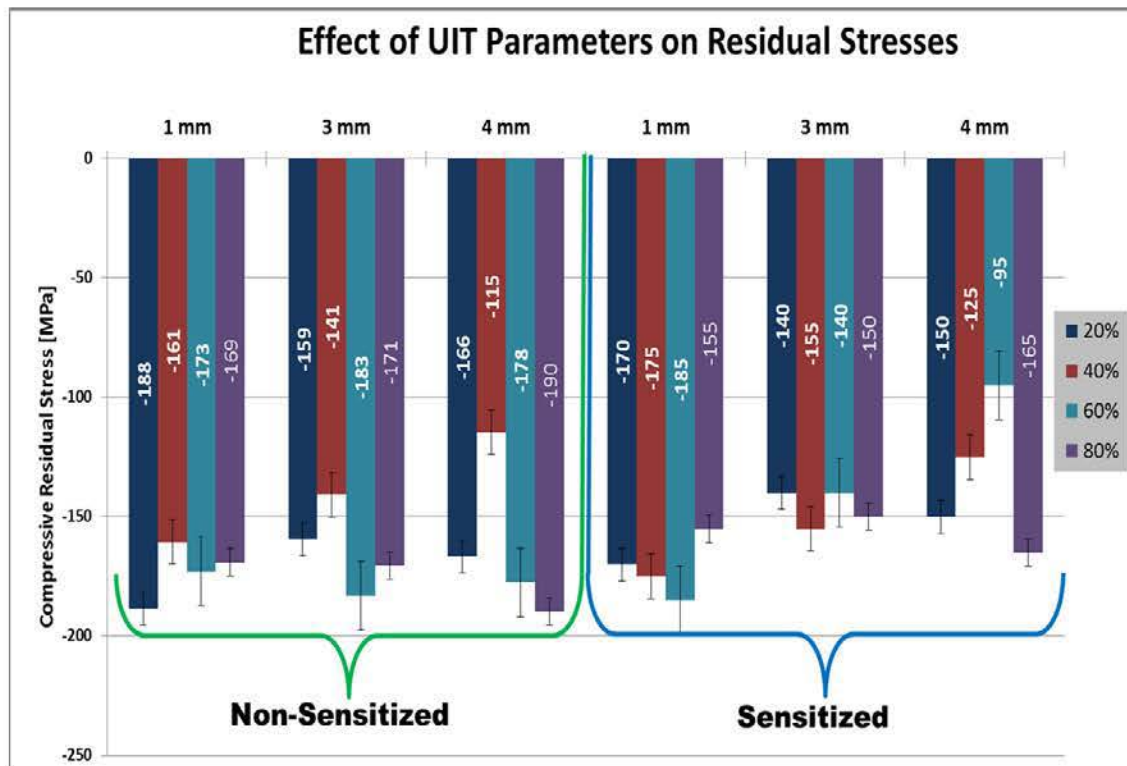
Figure 49. This chart compares average residual stresses generated in a region 10 to 100 mm from the toe of the weld under multiple UIT parameters on non-sensitized versus sensitized AA5456.[6]

---

[6] Data for the sensitized plates were roughly estimated from Figure 33 to Figure 36 [29].
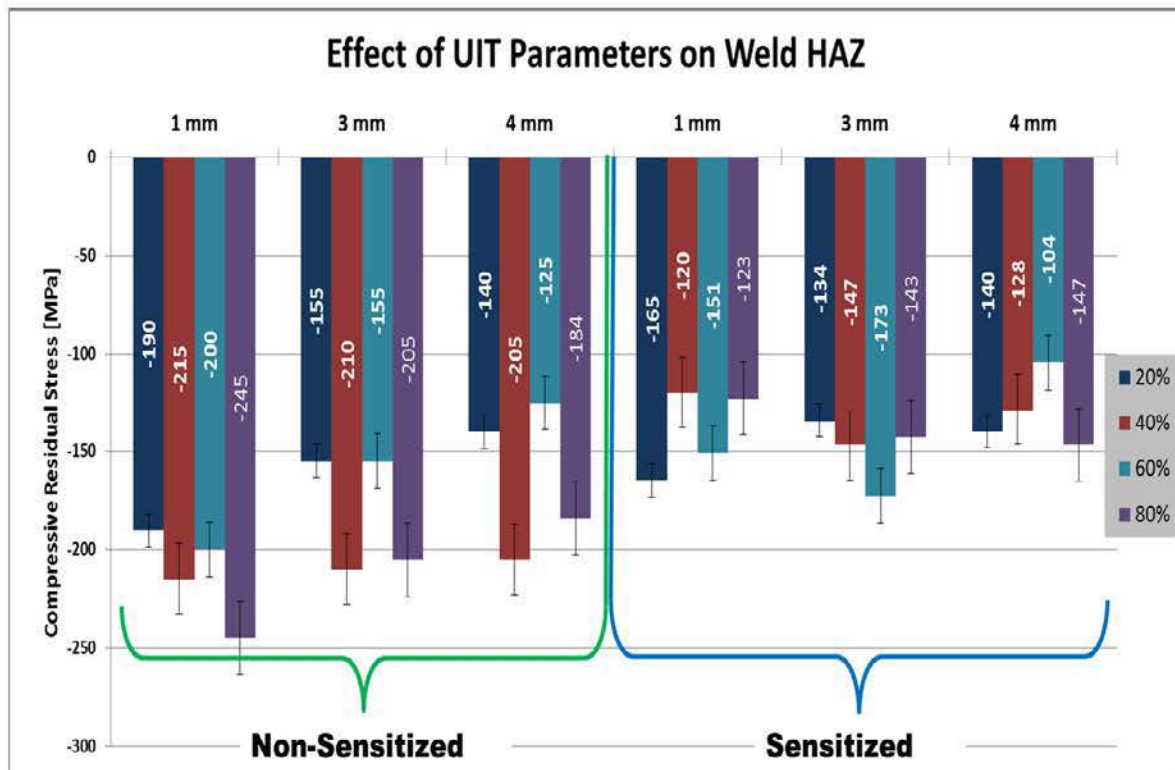
Figure 50. This chart compares average residual stresses generated from the toe of the weld out to 10 mm under multiple UIT parameters on non-sensitized versus sensitized AA5456.[7]

Upon optical microstructural analysis of the ultrasonic treated zones of all tested areas of the sensitized and non-sensitized AA5456 plates, extensive subsurface intergranular cracking was observed. Research performed by Castillo-Morales et al. [34] studied multiple combinations of UIT parameters and found that at specific amplitudes and pin sizes, microstructural subsurface cracking or tearing occurred in AA2024-T3. Of all the research conducted in this thesis, the discovery of extensive cracking in most of the ultrasonic treated zones of the **sensitized** plates was of most concern. The positive aspect of this discovery was through systematically comparing samples from each treated zone we were able to determine optimal UIT parameters required to not produce subsurface cracking. Using power input amplitude of 20 percent with a 3 mm or 4 mm pin and at amplitude of 60 percent with a 4 mm pin did not generate any subsurface

---

[7] Data for the sensitized plates were roughly estimated from Figure 33 to Figure 36 [29].

cracking. A pin size of 1 mm at any power input amplitude caused cracks to occur. This may be a result of excessive contact pressure due to the relatively small pin radius [13].

These results suggest a 20 percent input power, which is equivalent to amplitude of 12μm (see Table 3), with a 4 mm pin is the optimal UIT setting for all applications conducted on sensitized AA5456. Due to the compositional similarities between most 5XXX series AAs, specifically AA5083 used in newer and future U.S. naval combatants, it would also suggest using a lower UIT power amplitude and larger pin size. The use of a lower amplitude/power setting during the UIT process to minimize or reduce the risk of forming microstructural deformation is supported by Tran et al. [35]. Future research on sensitized AA5083 removed from a U.S. naval combatant, or sensitized in the laboratory, should be conducted using the same testing parameters and methods to validate these suggestions and compare the results to the sensitized AA5456 data. In contrast to the sensitized plates and to expected results, the **non-sensitized** plates showed **no** signs of cracking, tearing or any other type of microstructural deformation for any UIT parameter [34]. Further microstructural analysis of these samples by electron backscatter diffraction (EBSD) is recommended to verify the optical analysis results.

There is a general concern that metallography, consisting of grinding and polishing, could generate its own residual stresses on the surfaces of a metal. Some amount of grinding and polishing is required on ship structures, prior to x-ray diffraction-based residual stress measurements, in order to remove paint and other surface coatings; *In situ* metallography is now used on ship structures as an optical means for determining DOS in Al-Mg alloys [47]. The x-ray diffraction measurements taken on the *in situ* prepared, non-sensitized AA5083 plate show that some amount of compressive stress is generated during this process (see Figure 43 and Table 8). The compressive residual stresses were generated independent of particle size or if a polishing or grinding pad was used. Although the largest stress of -52.5 MPa was generated when grinding with the largest particle size, polishing with a 6 μm silica carbide solution produced a relatively comparable value of -45 MPa. These findings suggest that, for field-based measurements, electro polishing should still be used after mechanical polishing. In fact, the field x-ray diffraction measurements reported here may have some bias towards compressive values

because of the metallography; however, a contradiction to this suggestion was observed when residual stress measurements were taken at the forecastle of both polished and unpolished surfaces (see Figure 48). These measurements demonstrated that areas on the same weld with or without *in situ* metallography yielded similar values of residual stress. A more thorough investigation into the full effect *in situ* metallography has on residual stresses is necessary before any final conclusion is determined.

The complexity of ship structures requires a combination of weld modeling and simulation for full interpretation of residual stresses results. In simple butt welds of think or thick plates, the expected residual stress distribution can be analytically predicted and the same distribution is shown by x-ray residual stress measurements as observed by James et al.[25] and Haggett [13] (see Figure 29 through Figure 32). For the welded AA5083 plate strip in Mission Bay Area 1, tensile stresses were expected to be present from gas metal arc welding along these edges of the plate. The measured residual stresses, both longitudinal and transverse, were compressive in all areas (see Figure 45 through Figure 48). The ship geometry has several key differences from the simple free-standing plate. The AA5083 strip was welded on both sides. Stiffener plates had also been welded across the mission bay deck approximately 0.25 m away from the measurements. These added constraints and sources of residual stress must be taken into account when interpreting the x-ray residual stress.

Another example of the importance of combining experimental measurements of residual stress with simulation is the data from the deck-hull weld on the forecastle. Fisher and Sinfield at NSWCCD have modeled the expected residual stresses for this same weld. The field measurements showed compressive stresses although tensile stresses might be expected near the weld toe. As can be seen in the simulation, the maximum principal stresses are actually at a significant angle from the plane of the deck surface. In the future, we will perform combined simulations and residual stress experiments that can be compared directly. A suggestion from this thesis would be that a weld simulation be performed prior to performing field experiments in order to better design the field experiment and to give a sense of what results might be expected.

The driving motivation of this research was to determine if UIT can help prevent stress corrosion cracking (SCC) in welded sensitized AA5456. This thesis demonstrated that, at specific, optimal parameters of amplitude and pin size, UIT can assist in making 5XXX series AAs less susceptible to SCC by removing the tensile stress component. The findings of this research can dramatically change the procedures for how current and future ship repairs and maintenance are performed. With the continued push of extending the service life of U.S. naval combatants and the continued growing interest in using this series of aluminum in ship construction, these procedural changes have the potential of saving the U.S. Navy millions of dollars in man hours and material. More importantly, it can increase the operational readiness of critical strategic national defense resources.

V. CONCLUSION

This thesis used x-ray diffraction to characterize the effects of sensitization and ultrasonic impact treatment (UIT) on residual stresses in gas metal arc welded AA5456 plates. Optical microscopy was used to observe subsurface cracking created during systematically varied UIT conditions on the welded plates. Optimal UIT parameters, with respect to percent power input and pin diameter, were determined through the careful analysis of measured residual stress and observed microscopy data. The effect on residual stresses of industry standard surface preparation techniques was measured by XRD on a systematically in situ surface treated, non-sensitized AA5083 plate. X-ray diffraction was also used to perform field-based residual stress measurements of AA5083 installed on-board a U.S. naval combatant.

Thesis objectives and conclusions drawn from this research:

(1)   Assess the importance of UIT conditions, such as amplitude and pin diameter, on the level of elastic stress and plastic strain generated in AA5456.

- The UIT parameter of amplitude played less of role than pin size in the production of compressive residual stress in both the sensitized and non-sensitized AA5456 plates. Overall, UIT at all parameters evaluated in this thesis successfully produced uniform compressive stresses in the range of approximately -150 to -225 MPa, and neither pin diameter nor amplitude were the principal determining factor of how much compressive stress was produced. Residual stresses after UIT in the heat affected zones of sensitized plates were uniformly less compressive than for the non-sensitized plates.

(2)   Determine the role of sensitization in the generation of residual stresses and in the evolution of microstructure after UIT.

- Optimal UIT parameters required to prevent subsurface intergranular cracking in **sensitized** gas metal arc welded AA5456 were dependent on amplitude and pin diameter.
- No cracking was generated under three UIT conditions:
  - 20 percent power input (12μm amplitude) with a 3 or 4 mm pin
  - 60 percent power input (38μm amplitude) with a 4 mm pin

65

- No cracking was observed under any UIT condition for **non-sensitized** gas metal arc welded AA5456 plate.

(3)   Perform x-ray residual stresses on welded aluminum-alloy structures on a U.S. naval vessel.

- We successfully measured residual stresses in aluminum, welded structures on a U.S. Naval vessel using x-ray diffraction.
- *In situ* surface metallography may have a minor, but measurable effect on field-based x-ray diffraction residual stress measurements. An area of non-sensitized AA5083 plate went from a tensile residual stress of 11.8 MPa to a compressive stress of -23.5 MPa after *in situ* surface preparations to a 0.05 μm silica carbide polish was performed.
- Experimental residual stress measurements on ship structures should be combined with welding simulations to account for the complexity of ships structures in terms of the loadings and constraint.

LIST OF REFERENCES

[1]   L. Sawyer and W. Mitchell, *The Liberty Ships: The History of the "Emergency" Type Cargo Ships Constructed in the United States During the Second World War*, 2nd ed. London: Lloyd's of London Press, 1985.

[2]   N. Beavers and T. Lamb, "Aluminum benefits and advancements for naval ships," presented at the NSRP PDMT Panel Meeting, Pittsburgh, PA, 2010.

[3]   Y. Prawoto, K. Sumeru and W. Wan Nik, "Stress corrosion cracking of steel and aluminum in sodium hydroxide: Field failure and laboratory test," *Advances in Materials Sci. and Eng.,* vol. 2012, pp. 1–8, Jan. 2012.

[4]   R. Schwarting et al., "Manufacturing techniques and process challenges with CG47 class ship aluminum superstructure modernization and repairs," presented at the NSRP Ship Design and Materials Technol. Panel, Newport News, VA, 2011.

[5]   USS Chosin (CG-65). (2002, Jun. 19). *Wikipedia.* Available: http://en.wikipedia.org/wiki/USS_Chosin_%28CG-65%29. Accessed Mar. 11, 2015.

[6]   HSV-2 Swift. (2003, Nov. 4). *Wikipedia*. Available: http://en.wikipedia.org /wiki/HSV-2_Swift. Accessed Mar. 11, 2015.

[7]   USS Freedom. (2009, Dec. 2). Command Naval Surface Force, U.S. Pacific Fleet. [Online]. Available: http://www.public.navy.mil/surfor/lcs1/PublishingImages /uss-freedom.jpg

[8]   USS Independence drops anchor in St. Petersburg over holiday weekend. (2011, Aug. 09). Commander Naval Surface Force, U.S. Pacific Fleet. [Online]. Available: http://www.public.navy.mil/surfor/lcs2/Pages/USSIndependenceDrops AnchorinStPeterburgOverHolidayWeekend.aspx#.VQIQemOnHwE

[9]   D. Putnam, "Detection of heat sensitization in 5XXX-Series aluminum-alloys," Naval Sea Systems Command, Washington, DC, SBIR 2010.3, Topic N103-215, Sept. 2010.

[10]   R. Holtz et al., "Corrosion fatigue of AL 5083-H131 sensitized at 70, 100, and 175C and relation to microstructure and degree of sensitization," presented at NACE International DOD Corrosion Conference, La Quinta, CA, , 2011.

[11]   C. B. Crane and R. P. Gangloff, "Stress corrosion cracking of low temperature sensitized AA5083," presented at NACE International DOD Corrosion Conference, La Quinta, CA, 2011.

[12] *ASM Handbook on Properties and Selection: Nonferrous Alloys and Special-Purpose Materials*, vol. 2, Materials Park, OH: American Society of Materials International, 2012, pp. 3–61.

[13] M. Haggett, "Systematic review of UIT parameters on residual stresses of AA5456 and field based residual stress measurements predicting and mitigating stress corrosion cracking," M.S. thesis, Dept. Mech. Eng., Naval Postgraduate School, Monterey, CA 2014.

[14] Y. Zhong. (2005). Alloy phase diagram database. *ASM Alloy Phase Diagrams Center*. [Online]. Available: http://www1.asminternational.org.libproxy.nps.edu/asmenterprise/APD/ViewAPD.aspx?id=101029 Accessed Feb. 14, 2014.

[15] W.W. Sanders and K. A. McDowell, "Fatigue behavior of 5000 series aluminum alloy weldments in marine environment," in *Welding Research Council Bulletin*, no. 242, pp. 1–15, 1978.

[16] M. G. Fontana, *Corrosion Engineering*, New York: McGraw-Hill Book Company, 1987, pp. 820–824.

[17] R. Goswami et al., "Microstructural evolution and stress corrosion cracking behavior of Al-5083," in *Metallurgical and Materials Transactions*, vol. 42A, pp. 348–355, 2011.

[18] I. Oguocha, O. Adigun and S. Yannacopoulos, "Effect of sensitization heat treatment on properties of Al-Mg alloy AA5083-H116," *Journal of Material Sci.*, vol. 43, no. 12, pp. 4208–4214, 2008.

[19] D.S. Prasad et al. (2014, Jan.). Investigation on mechanical properties of aluminum hybrid composites. *Journal of Materials Research and Technology* [Online]. 3(1). Available: http://www.jmrt.com.br/en/investigations-on-mechanical-properties-of/articulo/90274157/

[20] E. C. Cormack, "The effect of sensitization on the stress corrosion cracking of aluminum alloy 5456," M.S. thesis, Dept. Mech. Eng., Naval Postgraduate School, Monterey, CA, 2012.

[21] F. Bovard, "Sensitization and environmental cracking of 5XXX aluminum marine sheet and plate alloys," presented at 198th Meeting of the Electrochemical , Pennington, NJ, 2004.

[22] N. Sukiman et al., "Durability and corrosion of aluminum and its alloys: overview, property space, techniques and developments," in *Aluminum Alloys—New Trends in Fabrication and Applications*, 2013, pp. 47–97.

[23] *Corrosion: Fundamentals Testing and Protection, Stress Corrosion Cracking*, vol. 13, Materials Park, OH, American Society of Materials International, 2012, pp. 346–366.

[24] M. James et al., "Residual stress and strain in MIG butt welds in 5083-H321 aluminum: as-welded and fatigue cycled," in *International Journal of Fatigue,* vol. 31, pp. 28–32, 2009.

[25] M. James et al., "Residual stress and strain in MIG butt welds in 5083-H321 aluminum: as-welded and fatigue cycled," in *International Journal of Fatigue,* vol. 31, pp. 34–40, 2009.

[26] V.M. Lihavainen et al., "Fatigue strength of a longitudinal attachment improved by ultrasonic impact treatment," in *Welding in the World,* vol. 48, no. 5–6, pp. 67–73, 2013.

[27] H. Zoeller and B. Cohen, "Shot peening for resistance to stress corrosion cracking," in *Metals Engineering Quarterly*, pp. 16–20, Feb. 1966.

[28] C. Rodopoulos et al., "The effect of surface engineering treatments on the fatigue behavior of 2024-T351 aluminum alloy," in *Journal of Materials Engineering and Performance,* vol. 16, no. 1, pp. 30–34, 2007.

[29] E. S. Statniko et al., "Comparison of ultrasonic impact treatment (UIT) and other fatigue life improvement methods," in *Welding in the World,* vol. 46, no. 3, pp. 20–32, 2002.

[30] X. An et al., "Study of the surface nanocrystallization induced by the esonix ultrasonic impact treatment on the near-surface of 2024-T351 aluminum alloy," in *Journal of Materials Engineering and Performance,* vol. 15, no. 3, pp. 355–364, June 2006.

[31] Europe Technologies Group. (2013, Oct.). STRESSONIC principle. [Online]. Available: http://www.sonats-et.com/page_12-stressonic.html

[32] Europe Technologies Group, (2009). Sonats needle peening objectives. [Online]. Available: http://www.sonats-et.com/page_23-needle-peening.html

[33] D. Goudar et al., "Measurement of residual stresses in surface treated stainless steel groove welds," in *Materials Science Forum,* vol. 681, pp. 49–54, 2011.

[34] M. Castillo-Morales and A. Salas-Zamarripa, "The effects of UIT in the fatigue life of Al 2024-T3," in *Key Engineering Materials,* vol. 449, pp. 15–22, 2010.

[35] M. Liao et al., "Effects of ultrasonic impact treatment on fatigue behavior of naturally exfoliated aluminum alloys," in *International Journal of Fatigue,* vol. 30, pp. 717–726, 2008.

[36]   K. N. Tran and L. Salamanca-Riba, "Microstructural evolution of severely plastically deformed sensitized aluminum 5456-H116 treated by ultrasonic impact treatment," in *Advanced Engineering Materials,* vol. 15, no. 11, pp. 1105–1110, 2013.

[37]   B. Mordyuk et al., "Enhanced fatigue durability of Al-6Mg alloy by applying ultrasonic impact peening: effects of surface hardening and reinforcement with AlCuFe quasicrystalline particles," in *Materials Science and Engineering A,* vol. 563, pp. 138–146, 2013.

[38]   X. Cheng et al., "Residual stress modification by post-weld treatment and its beneficial effect on fatigue strength of welded structures," in *International Journal of Fatigue,* vol. 25, pp. 1259–1269, 2003.

[39]   T. Okawa et al., "Effect of preload and stress ratio on fatigue strength of welded joints improved by ultrasonic impact treatment," in *Weld World,* vol. 57, pp. 235–241, 2013.

[40]   S. Ganguly et al., "Analysis of residual stress in metal-inert-gas-welded Al2024 using neutron and synchroton x-ray diffraction," in *Material Science Enginering Aluminum Structures,* vol. 491, no. 1, pp. 248–257, 2008.

[41]   S. Farrell et al., "Stress analysis on canadian naval platforms using a portable miniature x-ray diffractometer," in *Powder Diffraction,* vol. 25, no. 2, pp. 119–124, 2010.

[42]   B. Cullity, *Elements of X-ray Diffraction*, 3rd ed. Notre Dame, IN: Addison-Wesley, 1956.

[43]   I. Noyan and J. Cohen, *Residual Stress Measurement by Diffraction and Interpretation*, 1st ed. New York: Springer–Verlag, 1987.

[44]   *Manual for Stress Analysis-Software Manual.* Ontario, Canada: Proto Manufacturing Ltd., Oldcastle, 2010.

[45]   Naval Sea Systems Command, *Radialogical Affairs Support Program Manual* (SS0420-AA-RAD-010 Rev 1A). Washington Navy Yard, Naval Sea Systems Command, 2012.

[46]   Naval Postgraduate School, *NAVPGSCOL Instruction 6470.14: Standard and Emergency Operating Procedure for Proto iXRD*, Monterey, CA: Naval Postgraduate School, 2013.

[47]   W. Golumbfskie, private communication, "*In Situ* metallography," Mar. 2014.

INITIAL DISTRIBUTION LIST

1.   Defense Technical Information Center
        Ft. Belvoir, Virginia

2.   Dudley Knox Library
        Naval Postgraduate School
        Monterey, California